CONFIDENTIAL

RM L53J26

NACA RM L53J26

NACA

RESEARCH MEMORANDUM

LOW-SPEED INVESTIGATION OF THE EFFECTS OF LOCATION OF A DELTA AND A STRAIGHT TAIL ON THE LONGITUDINAL STABILITY AND CONTROL OF A THIN DELTA WING WITH EXTENDED DOUBLE SLOTTED FLAPS

By John M. Riebe and Jean C. Graven, Jr.

Langley Aeronautical Laboratory
Langley Field, Va.

CLASSIFIED DOCUMENT

NATIONAL ADVISORY COMMITTEE FOR AERONAUTICS

WASHINGTON

January 5, 1954

CONFIDENTIAL

NATIONAL ADVISORY COMMITTEE FOR AERONAUTICS

RESEARCH MEMORANDUM

LOW-SPEED INVESTIGATION OF THE EFFECTS OF LOCATION OF A DELTA AND A STRAIGHT TAIL ON THE LONGITUDINAL STABILITY AND CONTROL OF A THIN DELTA WING WITH EXTENDED DOUBLE SLOTTED FLAPS

By John M. Riebe and Jean C. Graven, Jr.

SUMMARY

A low-speed wind-tunnel investigation was made to determine the effects of horizontal-tail location and plan form on the longitudinal stability and control characteristics of a fuselage and a thin delta wing with extended double slotted flaps. The wing was a flat plate with beveled leading and trailing edges and had a maximum thickness ratio of 0.045 and 60° sweepback of the leading edge. The effects of a retractable canard horizontal surface to compensate for large diving moments of the extended double slotted flap were determined and an investigation was also made of an extended single slotted flap (Fowler-type flap).

The extended double slotted flap provided large values of untrimmed lift coefficient throughout the angle-of-attack range (1.05 at an angle of attack of 0° with a flap deflection of 61.3° and 1.94 at maximum lift with a flap deflection of 51.2°). Satisfactory locations of a 60° delta tail or a tail with an aspect ratio of 3.06, 23° 7' sweepback, and a taper ratio of 0.394 for longitudinal stability of the model with extended double slotted flaps deflected were indicated to be lower and further to the rear than for flap-undeflected conditions.

Tail-incidence tests indicated that the delta tail (which had 20 percent of the wing area) or the tail with a taper ratio of 0.394 (14.5 percent of the wing area) would be incapable of providing longitudinal trim with the extended double slotted flap because of a large diving moment resulting from flap deflection. The use of larger tails at a tail length of two wing mean aerodynamic chords would result in estimated trim lift

coefficients of 0.72 and 1.67 at an angle of attack of 0° and maximum lift, respectively. The delta tail was generally found to be superior with regard to stability and control to the tail with a taper ratio of 0.394. (Both tails had approximately the same variation of lift with angle of attack.) The addition of a retractable canard horizontal surface (that was intended to be extended simultaneously with the flaps so that trim could be effected by the all-movable delta tail) generally resulted in a longitudinally stable high-lift delta-wing airplane configuration with a trim lift coefficient of 0.82 at an angle of attack of 0° and a maximum trim lift coefficient of 2.30. The increase in maximum lift coefficient and angle of attack for maximum lift with the addition of the canard to the delta-wing model is believed to have resulted largely from canard-surface wake effects on the wing. Trim lift coefficients for the extended single slotted flap were estimated to be 0.41 at an angle of attack of 0° and 1.56 at maximum lift.

INTRODUCTION

Investigations made by the National Advisory Committee for Aeronautics (refs. 1 to 4) have shown that large increments of trim lift coefficient can be obtained on delta-wing airplanes by the use of double slotted flaps and static longitudinal stability can be maintained up to the stall by the use of a horizontal tail located at the proper position. These large lift increments were obtained, however, in the low and moderate angle-of-attack range and only relatively small gains in maximum lift coefficient were obtained because of a reduction of flap effectiveness at high angles of attack.

The results of an investigation of a modified double slotted flap configuration which provides large gains in lift coefficient throughout the entire working angle-of-attack range and the effects of tail location and plan form on the longitudinal stability and control of the configuration are given in the present paper. The flap arrangement, which will be called the extended double slotted flap, differs from the conventional double slotted flap configuration in that the flap and vane are displaced to the trailing edge of the wing (similar to Fowler flaps) in addition to being rotated to a given flap deflection. Tail configurations tested were a 60° delta tail and a tail with an aspect ratio of 3.06, taper ratio of 0.394, and 23° 7' sweepback of the leading edge. Both tails had approximately the same variation of lift with angle of attack. Included in the present paper are the results of an exploratory investigation of a retractable canard horizontal surface (hereafter called a canard) which could be used to trim (with an increase of lift coefficient) the diving moment

which accompanies extended double slotted flap deflection. Results are also presented of a limited investigation of a Fowler-type flap on the delta wing.

COEFFICIENTS AND SYMBOLS

The results of the tests are presented as standard NACA coefficients of forces and moments about the stability axes. The positive directions of forces, moments, and angles are shown in figure 1. Pitching-moment coefficients are given about the wing 25-percent-mean-aerodynamic-chord point shown in figure 2. The coefficients and symbols are defined as follows:

C_L lift coefficient, L/qS

C_D drag coefficient, D/qS

C_m pitching-moment coefficient, $M/qS\bar{c}$

L lift, lb

D drag, lb

M pitching moment, ft-lb

q free-stream dynamic pressure, $\frac{1}{2}\rho V^2$, lb/sq ft

S wing area, 6.93 sq ft (See fig. 2)

$\bar{c}$ wing mean aerodynamic chord, 2.31 ft, $\frac{2}{S}\int_0^{b/2} c^2\,dy$ (See fig. 2)

b wing span, 4.00 ft (See fig. 2)

V free-stream velocity, ft/sec

ρ mass density of air, slugs/cu ft

δ_f flap deflection measured in plane perpendicular to hinge line, deg

δ_v vane deflection measured in plane perpendicular to hinge line, deg

α angle of attack of wing, deg

c local wing chord, ft

y lateral distance from plane of symmetry measured parallel to Y-axis, ft

z vertical location of tail with respect to chord line extended, positive when located above chord line extended

l distance of tail-quarter-chord position back of wing quarter-chord position

i_t incidence of horizontal tail, deg

i_c incidence of canard, deg

ϵ effective downwash angle, deg

Subscripts:

max maximum

t horizontal tail

MODEL AND APPARATUS

The model was tested on a single-support strut in the Langley 300 MPH 7- by 10-foot tunnel.

The 60° delta wing (fig. 2(a) and table I) was the same as that used in references 1 to 3 with the exception of rounded tips and a more outboard location of the flaps (flaps in present investigation extended from 0.18b/2 to 0.74b/2). The wing was made from a flat steel plate 5/8 inch thick with beveled leading and trailing edges. The thickness varied from 0.015c at the root to a maximum of 0.045c near 0.67b/2. The mahogany fuselage had the same geometry as that used in the Langley unified wing program for supersonic flight.

The extended double slotted flap (fig. 2(b) and tables II and III) was obtained by displacing the vane and flap to the trailing edge of the

wing and by using the same vane-flap-gap configuration as that of the double slotted flap configuration of reference 2. The extended single slotted flap configuration (similar to a Fowler flap) had the same gap arrangement as that of the single slotted flap of reference 2.

The various tail configurations tested on the model are shown in figure 2(c). The delta tail (fig. 2(c)) was constructed of 1/4-inch sheet aluminum with geometric characteristics similar to those of the delta wing and had an area which was 20 percent of the wing area. The straight tail (14.5 percent of the wing area) had an aspect ratio of 3.06, a taper ratio of 0.394 and a double wedge airfoil section; construction was of aluminum. Both tails had approximately the same variation of lift with angle of attack. The tail was located at the different longitudinal positions by means of interchangeable fuselage afterbody blocks; positioning above and below the wing chord line extended (fig. 2(c)) was accomplished by supporting the tail on 1/2-inch steel vertical struts (fig. 2(a)). The canard arrangement tested on the model (fig. 3), which represented a retractable surface, was constructed of 1/8-inch sheet aluminum having the same plan-form dimensions as the delta tail of figure 2(b).

TESTS

The tests were made at a dynamic pressure of approximately 25 pounds per square foot, corresponding to an airspeed of about 100 miles per hour. Reynolds number for this airspeed based on the mean aerodynamic chord (2.31 feet) was approximately 2.2×10^6. The corresponding Mach number was 0.13. Angles of attack ranged from -15° to 33°. Tests were made with the tail with a taper ratio of 0.394 located on and $0.75\bar{c}$ above the wing chord line extended at $1.0\bar{c}$ and $1.5\bar{c}$ behind the $0.25\bar{c}$ location and also on and $0.25\bar{c}$ below the wing chord line extended at a tail length of $2.0\bar{c}$ (fig. 2(c)). The delta tail was located on, $0.25\bar{c}$ above, and $0.25\bar{c}$ below the wing chord line extended at a tail length of $2.0\bar{c}$ (fig. 2(c)).

CORRECTIONS

Jet boundary corrections, obtained from methods outlined in reference 5, have been applied to the angle of attack, the drag coefficient, and the tail on pitching-moment coefficient. Blocking corrections have been applied to the model according to the method of reference 6. A buoyancy correction has been applied to the model to account for a longitudinal static-pressure gradient in the tunnel.

RESULTS AND DISCUSSION

Presentation of Data

The data obtained are presented in the following figures:

Flap Arrangements, Tail Off

Effect of extended double slotted flap deflection.- Large increments of lift were obtained throughout the lift-coefficient range up to and including $C_{L_{max}}$ for the extended double slotted flap (fig. 4). The lift coefficient at an angle of attack of 0° for the extended double slotted flap was only slightly larger than the lift coefficient for the double slotted flap of reference 4 throughout the comparable flap-deflection range (46° to 57°) (fig. 6). Flap effectiveness, however, held to higher deflection angles for the extended double slotted flap than for the double slotted flap. The lift increment at an angle of attack of 0° for the extended double slotted flap was 1.05 (for 61.3° flap deflection, the highest tested) compared with 0.925 for the double slotted flap (at a deflection of about 57° which the trend of the lift curve with flap deflection indicates is very nearly the optimum deflection). Extension of the double slotted flap to the wing trailing edge became much more beneficial with regard to lift-coefficient increment as the angle of attack was increased. At an angle of attack of 10°, the extension of the double slotted flap to the trailing edge resulted in an increment of 0.30 lift coefficient so that a lift coefficient of 1.55 was produced;

at $C_{L_{max}}$ the increment was almost 0.40 resulting in a maximum lift coefficient of 1.94. The increased lift at high angles of attack for the flap-extended configuration can be attributed to the larger lifting area compared with the double slotted flap configuration (which results in increased lift-curve slope when basing the coefficients on the flap-retracted wing area) and also to the elimination of the nonlinearity of the lift curve at high angles of attack. Approximately half the difference between maximum lift coefficients of the double slotted and extended double slotted flap configurations can be attributed to the latter cause.

Larger diving moments accompanied the increased lift of the double slotted flap when extended to the wing trailing edge so that, when compared on a trimmed-lift-coefficient basis, maximum lift coefficients were closer: 1.40 for the double slotted flap and 1.63 for the extended double slotted flap for a tail length of $2.0\bar{c}$ and with flap deflections of about 52°.

Studies of the air flow over the surface of delta wings with double slotted flaps by means of wool tufts have indicated that the flow over the part of the wing ahead of the flap generally becomes unstable and separates earlier than the flow over the flaps. Reduction of lift-curve slope at high angles of attack for double slotted flaps (refs. 1 to 4) possibly may have resulted from additional load over the wing from the flap precipitating early wing stall. Although no pressure or tuft studies have been made thus far to provide evidence, it is thought that the more linear lift curve with the extended double slotted flap (fig. 4) might be attributed to the larger wing area ahead of the flap which can carry the additional loading from the flap to high angles of attack without separating.

In the high-lift-coefficient range, lift-drag ratios for the wing with extended double slotted flap were larger than that of the wing with flap retracted (fig. 4). Comparison with the data of reference 4 also indicates that above about 1.3 lift coefficient the extended double slotted flap had equal or larger lift-drag ratios than double slotted flaps.

Effect of extended single slotted flap deflection.- A lift-coefficient increment of 0.55 at an angle of attack of 0° was obtained for the extended single slotted flap at a deflection of 35° (figs. 5 and 6). An increase of flap deflection to about 40° generally resulted in only a very slight increase in lift coefficient. Throughout comparable flap-deflection ranges the extended single slotted flap gave larger increments of lift at an angle of attack of 0° than the single slotted flap of reference 2. However, at a given lift coefficient the diving moment resulting from extended single slotted flap deflection was larger than that resulting from deflection of the single slotted flap of reference 2.

Additional down load on the tail required to trim the larger diving moment would reduce the difference in lift coefficient for the two flaps at a given angle of attack. Trim lift coefficients for the model with the extended single slotted flap and with a horizontal tail at $2.0\bar{c}$ were estimated from the tail-off tests to be 0.41 and 1.56 at an angle of attack of 0° and maximum lift, respectively.

Extended Double Slotted Flaps

Effect of location of the delta tail on longitudinal stability.- A previous investigation of the effect of location of the delta tail on the model with delta wing and double slotted flaps (ref. 4) has shown that the most satisfactory tail locations for longitudinal stability were at rearward positions on the chord line extended or at positions below the chord line extended. Delta-tail tests for the present investigation with extended double slotted flaps (fig. 7) were therefore restricted to the rearward positions ($l = 2.0\bar{c}$). The results were similar to those of reference 4: a longitudinally stable configuration occurred with the delta tail located on or below the chord line extended and longitudinal instability resulted when the delta tail was located above the chord line extended (figs. 7 and 11). The approximate region (determined largely from ref. 7) at which location of delta tails behind delta wings with flaps zero resulted in nonlinearity of the pitching-moment-coefficient curve and longitudinal instability over part of the lift-coefficient range is included in figure 11.

With the tail off, the extended double slotted flap model had an unstable break of the pitching-moment curve at high angles of attack. As was concluded in reference 4 with double slotted flaps and in reference 7 with flaps zero, longitudinally stable locations of the delta tail behind the delta wing with the extended double slotted flaps can be attributed to regions of stabilizing downwash effect at high angles of attack resulting from vortex flow behind delta wings. Changes in dynamic pressure at the tail were found in reference 7 to have a minor effect.

Control effectiveness of the delta tail at locations for longitudinal stability.- When located at positions for longitudinal stability ($l = 2.0\bar{c}$ with $z = -0.25\bar{c}$ and 0, figs. 8(a) and 8(b), respectively) the delta tail would probably be incapable of providing longitudinal trim in the high-lift-coefficient range for the model with extended double slotted flaps. The effectiveness of the delta tail with extended double slotted flaps was about the same as that with double slotted flap of reference 4. The large diving moment resulting from deflection of the extended double slotted flap, however, requires tail lift coefficients for longitudinal trim at high angles of attack which are beyond the capabilities of the delta tail. The large diving moments near maximum lift (C_m approximately -0.66 tail off) would require a down load when trimmed in pitch for

$l = 2.0\bar{c}$ which would reduce $C_{L_{max}}$ from 1.99 to 1.66. (Slight differences in estimated trim lift coefficients here and given previously are caused by different tail-off fuselage lengths.)

Effect of location of the tail with a taper ratio of 0.394 on longitudinal stability.- The effect of location of the tail with a taper ratio of 0.394 on the longitudinal stability of the model with extended double slotted flaps (fig. 9) was somewhat similar to the stability characteristics of the model with the delta tail and either extended double slotted (fig. 7) or double slotted flaps (ref. 4); that is, tail positions above the chord line extended were longitudinally unstable over part of the angle-of-attack range and rearward tail positions on and below the chord line extended were generally longitudinally stable (fig. 11). However, almost neutral stability existed in the intermediate angle-of-attack range ($\alpha = 0^\circ$ to 8°) when the tail with a taper ratio of 0.394 was located on the chord line extended and an unstable break occurred at the stall when located below the chord line extended. Corresponding location for the delta tail with about the same incidence angle showed only slight reduction in stability at the intermediate angles of attack and a stable pitching-moment break at the stall. Both tail plan forms produced about the same longitudinal stability in the low angle-of-attack range. The difference in stability at the other lift coefficients might be attributed to the disposition of the area of the two plan forms. With the tail mean aerodynamic quarter chord at the same position, the tail with a taper ratio of 0.394 has a large part of its area more forward and more outboard than the area of the delta tail. A large area of the tail with a taper ratio of 0.394 is thus effectively in a lateral location where with increasing angle of attack it is more difficult to get out of a region of high downwash into low downwash as the horizontal tail traverses across the large trailing vortices which occur behind the delta wing. As shown in figure 15 which gives effective downwash angles for the two tail plan forms, the stabilizing region of the variation of downwash angle with angle of attack starts at higher angles of attack for the tail with a taper ratio of 0.394 than for the delta tail.

Control effectiveness of the tail with a taper ratio of 0.394 at optimum locations for stability.- The tail with a taper ratio of 0.394 was unable to provide longitudinal trim at any lift coefficient when located at one of the more favorable positions for longitudinal stability (tail length of $2.0\bar{c}$ on the wing chord line extended, fig. 10). As with the delta tail, this deficiency resulted from the large diving moment with deflection of the extended double slotted flap which required lift loads beyond the capabilities of the tail. Practically no pitching-moment effectiveness was present for negative tail-incidence angles and this lack of effectiveness probably resulted from the high effective downwash angle (fig. 15) and the lower stall angle of attack for the straight tail than for the delta tail.

Canard With Extended Double Slotted Flap and Delta Tail

A possible method of obtaining longitudinal trim and the high lift coefficients of the extended double slotted flap arrangement at high angles of attack and of using the large diving moments (accompanying extended double slotted flap deflection) to an advantange would be the use of a canard surface which would be retracted inside the fuselage for the clean flight condition and extended when the extended double slotted flaps were deflected. Such an arrangement would provide an addition to lift and a nose-up moment to the airplane. An arrangement that might be used is shown in figure 16, which is a sketch of a delta-wing airplane with extended double slotted flaps in the landing condition as seen from below. The front landing-gear doors have been opened laterally to a horizontal position in order to provide additional lift and nose-up moment to the airplane. Unpublished tests in the Langley 300 MPH 7- by 10-foot tunnel have shown that delta wings which are portions of a cone (as are the doors in the sketch) will provide lift comparable to straight delta wings. For simplification of testing a retractable canard arrangement has been simulated in the present investigation by a delta wing mounted at the fuselage nose (fig. 3).

Effect of canard incidence.- The canard had pronounced effects on both the lift and pitching moment of the model with extended double slotted flaps. The addition of the canard increased the maximum lift coefficient and extended the angle of attack for maximum lift (fig. 12). The canard at an incidence angle of 10° had the largest effect so the maximum lift coefficient was increased from 1.95 to 2.45 and the angle of attack for maximum lift was extended from 23° to 30°. However, throughout most of the extended angle-of-attack range, the model had large longitudinal instability. Smaller increases in maximum lift coefficient occurred for the higher canard incidence angles. However, a reduction of the longitudinal instability in the high angle-of-attack range occurred with increased canard incidence so that with $i_c = 25°$ the high-angle-of-attack instability was restricted to a small lift-coefficient range. As shown in figure 12 the increment of lift resulting from addition of the canard was greater at high angles of attack than at low angles of attack. For example, the addition of the canard at 20° incidence increased the lift coefficient 0.17 at an angle of attack of 9°; however, at an angle of attack of 24° the increase in lift coefficient was 0.4. With canard off the lift coefficient decreased with angle of attack beyond approximately an angle of attack of 23°. The increase of lift coefficient with angle of attack beyond 23° when the canard surface was added to the model cannot be attributed entirely to increased lift on the canard alone but probably resulted from an effect of the canard on the wing lift. This effect can be noted from figure 12 which shows an increase of lift coefficient when model angle of attack was increased but shows no increase or a decrease in lift when canard incidence was increased

(beyond $i_c = 10^\circ$). This result suggests that the vortex wake from the canard surface is having an effect on the lift of the wing itself and will probably result in a more favorable lift distribution on the wing. A similar increase in maximum lift coefficient with the addition of a canard tail to a delta wing with flaps zero, although not discussed, was found in the data of reference 8.

The addition of the canard to the delta-wing model resulted in a nonlinearity of the lift-coefficient curve in the angle-of-attack range near zero, particularly for the configuration with the canard at 25° incidence. Canard deflections beyond 15° provided only small change in pitching-moment coefficient beyond an angle of attack of 10°. Canard effectiveness fell off when the total of the model angle of attack and canard incidence angle was greater than 25°. This result might be expected because the stall angle of delta wings with flaps zero is near the region of 30°. However, part of the apparent drop-off in pitching-moment effectiveness at high incidence angles might be caused by a reduction of canard vortex effect on the main wing. If the stable pitching-moment curve with the high canard incidence angle is caused primarily from separation of air flow over the canard, dynamic longitudinal stability deficiencies might result for an airplane with such an arrangement. In the case of rapid pull-up, canard stall might be momentarily delayed and might result in pitch-up of the airplane.

Effect of delta-tail incidence with fixed canard.- For the three configurations for which delta-tail effectiveness was investigated at a tail length of $2.0\bar{c}$ ($z = 0$ and $-0.25\bar{c}$ with $i_c = 20^\circ$, figs. 13(a) and 13(b), respectively, and $z = -0.25\bar{c}$ with $i_c = 25^\circ$, fig. 13(c)), longitudinal trim could be obtained throughout the angle-of-attack range. Maximum trim lift coefficients obtainable ranged from 2.0 to about 2.3 depending on test arrangement.

Longitudinal instability occurred below a lift coefficient of 1.5 for the configuration with the canard at 20° and the tail located on the chord line extended (figs. 13(a) and 14). More satisfactory longitudinal stability resulted when the tail was located below the wing chord line extended (fig. 13(b)). However, for this configuration slight longitudinal instability occurred near maximum lift coefficient and longitudinal instability was also present at low lift coefficients corresponding to the negative angle-of-attack range. Some improvement in longitudinal stability was effected by reducing the flap deflection from 56.2° to 51.2° so that the flap diving moment was reduced and thus the required negative tail incidence. The most satisfactory arrangement tested with regard to longitudinal stability occurred with the canard fixed at 25° and with the tail located below the wing chord line extended (fig. 13(c)). The maximum trim lift coefficient available for the $i_c = 25^\circ$ configuration was about 2.0; the maximum lift coefficient obtained with $i_c = 20^\circ$ was 2.3.

The pitching-moment break at the stall was stable with $i_c = 25^\circ$ and longitudinal stability was present at angles of attack to at least zero and may exist at negative angles but lack of i_t for trim data prevents actual determination in the negative angle-of-attack range.

CONCLUSIONS

A low-speed wind-tunnel investigation to determine the effect of an extended double slotted flap and horizontal-tail location and plan form on the lift, longitudinal stability, and longitudinal control characteristics of a thin delta-wing fuselage model indicates the following conclusions:

1. Large values of untrimmed (tail-off) lift coefficient (1.05 at zero angle of attack and 1.94 at maximum lift) were obtained throughout the working angle-of-attack range with the extended double slotted flap. Estimated trimmed lift coefficients for the model with a tail length of $2.0\bar{c}$ and a flap deflection of 56.2° were 0.71 at an angle of attack of 0° and 1.64 at maximum lift.

2. Satisfactory location of a 60° delta tail or a tail with an aspect ratio 3.06, 23° 7' sweepback of the leading edge, and a taper ratio of 0.394 for longitudinal stability of the model with extended double slotted flaps was generally at rearward positions on the wing chord line extended or at positions below the chord line extended.

3. Tail-incidence tests indicated that the delta tail (which had 20 percent of the wing area) or the tail with a taper ratio of 0.394 (14.5 percent of the wing area) would be incapable of providing longitudinal trim with the extended double slotted flap because of a large diving moment resulting from flap deflection.

4. The delta-plan-form tail was generally found to be superior with regard to stability and control than the tail with a taper ratio of 0.394. (Both tails had approximately the same variation of lift with angle of attack.)

5. Investigation of a retractable canard, that was intended to be extended simultaneously with deflection of the extended double slotted flap, resulted in a generally longitudinally stable high-lift delta-wing airplane configuration with a trim lift coefficient of 0.82 at an angle of attack of 0° and a maximum trim lift coefficient of 2.3.

6. The increase in maximum lift coefficient and angle of attack for maximum lift with the addition of the canard to the delta-wing model is believed to have resulted largely from canard-surface wake effects on the wing lift.

7. Trim lift coefficients of the model with an extended single slotted flap and a horizontal-tail length of twice the mean aerodynamic chord were estimated from tail-off tests to be 0.41 and 1.56 at an angle of attack of 0° and maximum lift, respectively.

Langley Aeronautical Laboratory,
National Advisory Committee for Aeronautics,
Langley Field, Va., October 15, 1953.

REFERENCES

1. MacLeod, Richard G.: A Preliminary Low-Speed Wind-Tunnel Investigation of a Thin Delta Wing Equipped With a Double and a Single Slotted Flap. NACA RM L51J26, 1952.

2. Riebe, John M., and MacLeod, Richard G.: Low-Speed Wind-Tunnel Investigation of a Thin Delta Wing With Double Slotted, Single Slotted, Plain, and Split Flaps. NACA RM L52J29, 1953.

3. Riebe, John M.: The Effects of Fuselage Size on the Low-Speed Longitudinal Aerodynamic Characteristics of a Thin 60° Delta Wing With and Without a Double Slotted Flap. NACA RM L52L29a, 1953.

4. Riebe, John M., and Graven, Jean C., Jr.: Low-Speed Investigation of the Effects of Location of a Delta Horizontal Tail on the Longitudinal Stability and Control of a Fuselage and Thin Delta Wing With Double Slotted Flaps Including the Effects of a Ground Board. NACA RM L53H19a, 1953.

5. Gillis, Clarence L., Polhamus, Edward C., and Gray, Joseph L., Jr.: Charts for Determining Jet-Boundary Corrections for Complete Models in 7- by 10-Foot Closed Rectangular Wind Tunnels. NACA WR L-123, 1945. (Formerly NACA ARR L5G31.)

6. Herriot, John G.: Blockage Corrections for Three-Dimensional-Flow Closed-Throat Wind Tunnels, With Consideration of the Effect of Compressibility. NACA Rep. 995, 1950. (Supersedes NACA RM A7B28.)

7. Jaquet, Byron M.: Effects of Horizontal-Tail Position, Area, and Aspect Ratio on Low-Speed Static Longitudinal Stability and Control Characteristics of a 60° Triangular-Wing Model Having Various Triangular-All-Movable Horizontal Tails. NACA RM L51I06, 1951.

8. Newman, Ernest E., and Cahill, Jones F.: Investigation at Low Speed of the Flow Field Behind the Lifting Surfaces of a Model Equipped With a 60° Triangular Wing and a 60° Triangular Canard Tail. NACA RM L53C30, 1953.

TABLE I.- PHYSICAL CHARACTERISTICS OF THE TEST MODEL

Wing:	
Span, ft	4.00
Aspect ratio	2.31
Thickness of flat plate (maximum thickness ratio, 0.045) in.	5/8
Sweep, deg	60.00
Area, sq ft	6.93
Mean aerodynamic chord, ft	2.31
Leading-edge bevel angle, deg	6.8
Taper ratio	0
Vane:	
Span, ft	2.98
Chord, ft	0.13
Chord, percent wing root chord	3.6
Chord, percent flap chord	27.3
Flap:	
Span, ft	2.98
Chord, ft	0.46
Chord, percent wing root chord	13.2
Area, sq ft	1.03
Area, percent wing area	14.83
Trailing-edge bevel angle, deg	8.00
Delta tail:	
Span, ft	1.79
Aspect ratio	2.31
Thickness of flat plate (maximum thickness ratio, 0.045) in.	0.25
Sweep, deg	60.00
Area, sq ft	1.39
Area, percent wing area	20.0
Mean aerodynamic chord, ft	1.03
Leading-edge bevel angle, deg	6.0
Trailing-edge bevel angle, deg	7.3
Taper ratio	0
Tail with a taper ratio of 0.394:	
Span, ft	1.75
Aspect ratio	3.06
Thickness ratio	0.045
Sweep, deg	23° 7'
Area, sq ft	1
Area, percent wing area	14.5
Mean aerodynamic chord, ft	0.61

TABLE II.- ORDINATES OF THE VANE

[All dimensions are in inches]

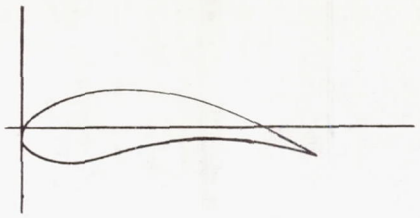

Station	Lower surface	Upper surface
0	0	0
.025	-.067	.051
.075	-.105	.100
.125	-.125	.130
.175	-.139	.153
.225	-.145	.175
.275	-.145	.190
.325	-.138	.205
.400	-.125	.219
.500	-.099	.221
.600	-.074	.215
.700	-.055	.205
.800	-.044	.180
.900	-.039	.153
1.000	-.042	.115
1.100	-.050	.075
1.200	-.066	.025
1.300	-.083	-.032
1.400	-.105	-.083
1.500	-.153	-.153

TABLE III.- ORDINATES OF THE LEADING EDGE OF THE TRAILING-EDGE FLAP

[All dimensions are in inches]

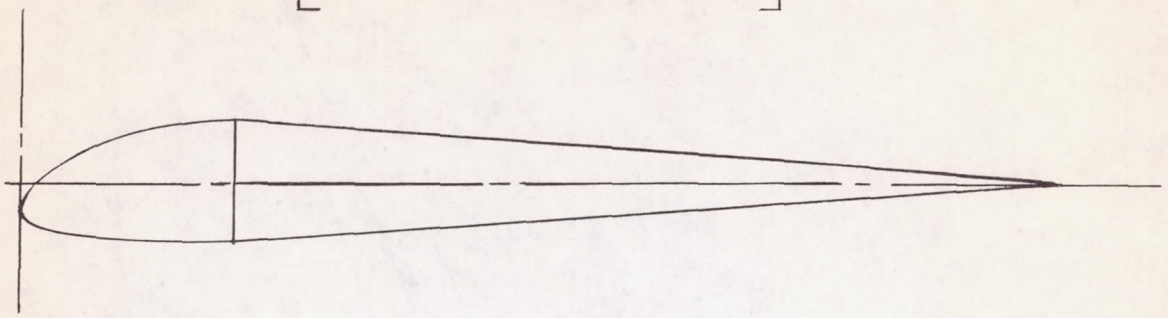

Station	Upper surface	Lower surface
0	-0.15	-0.15
.1	.01	-.25
.2	.08	-.27
.4	.18	-.29
.6	.25	-.30
.8	.30	-.31
1.1	.31	-.31

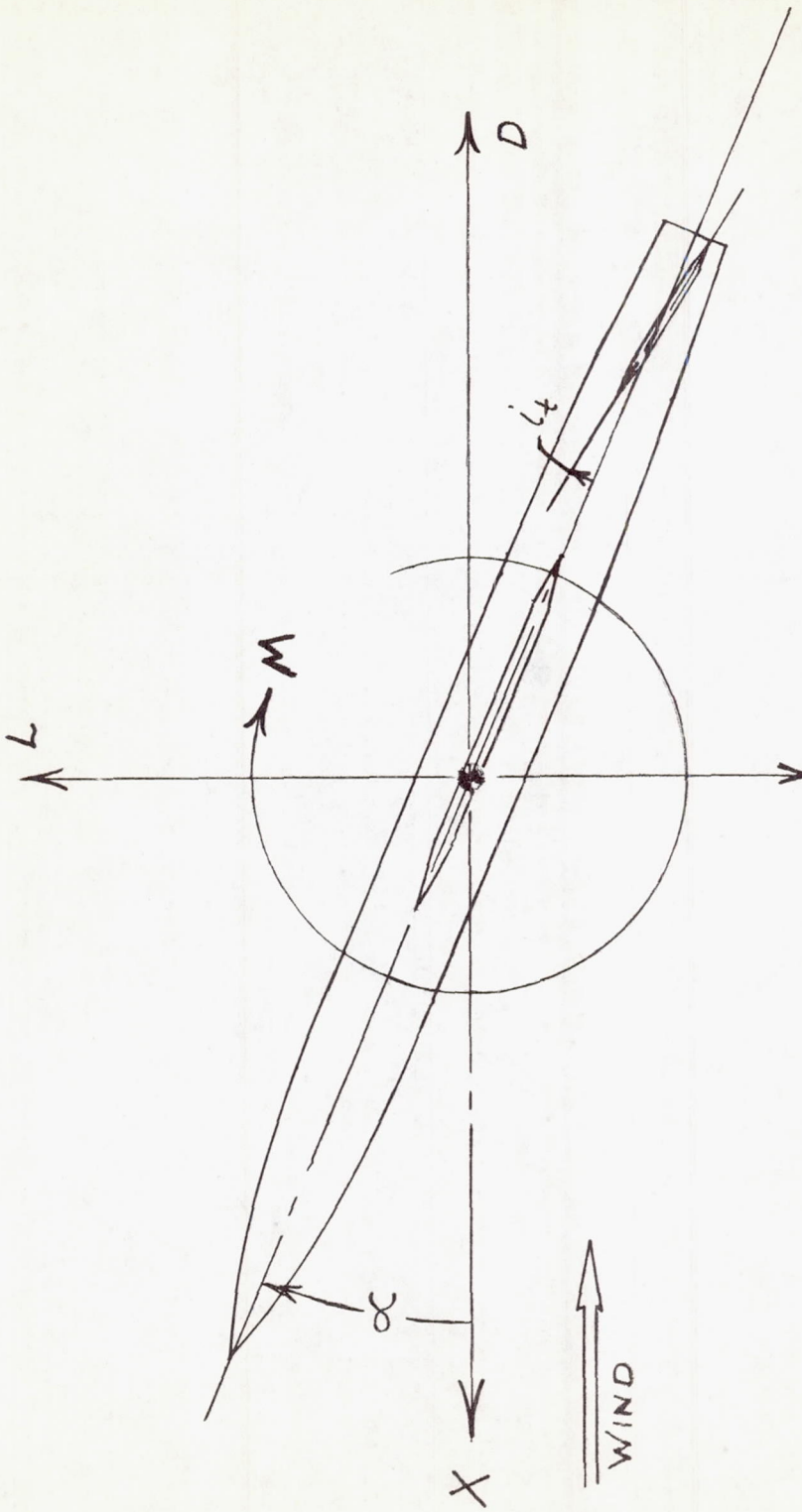

Figure 1.- System of stability axes. Positive values of forces, moments, and angles are indicated by arrows.

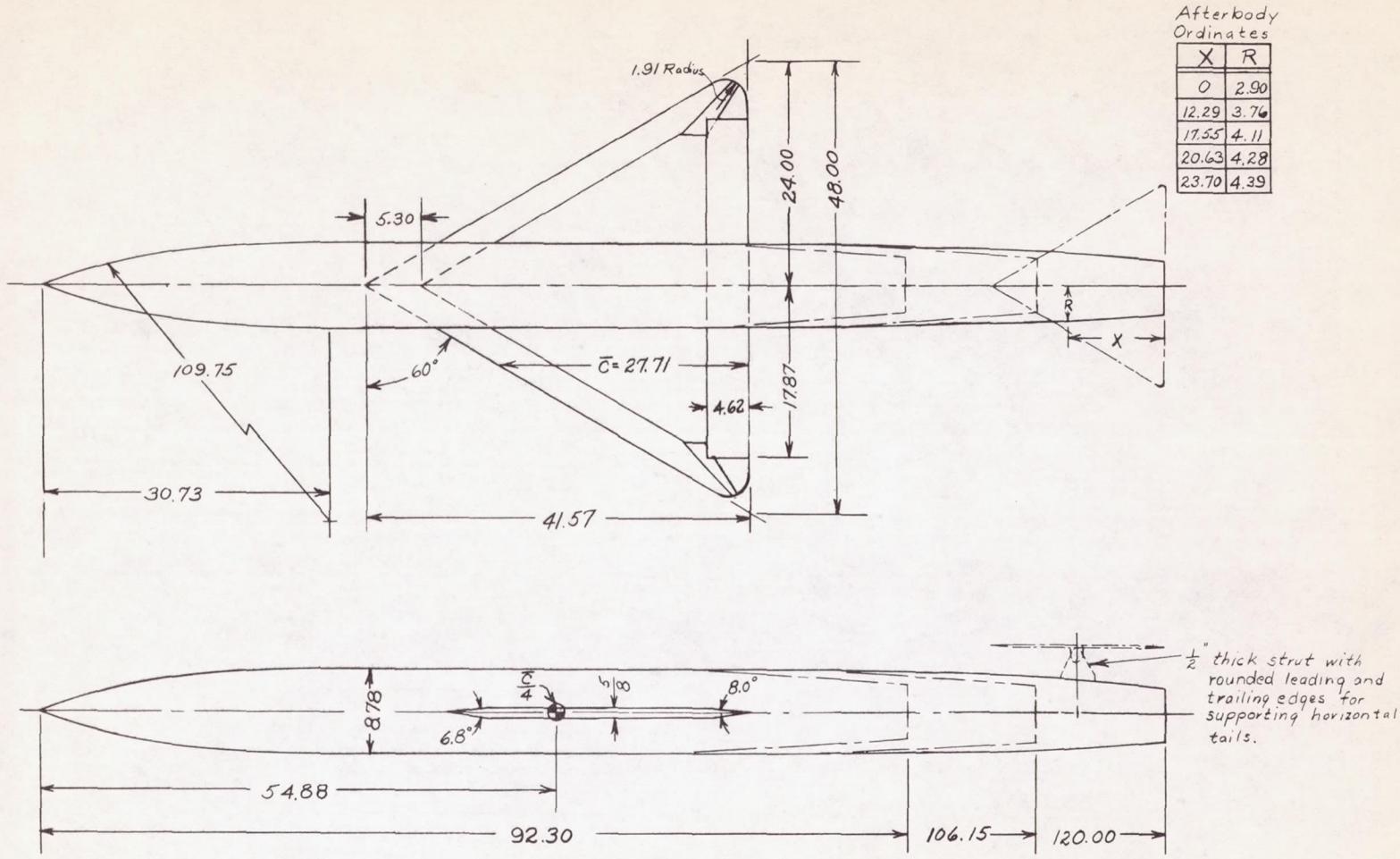

(a) Details of fuselage and wing.

Figure 2.- General arrangement of the wing, fuselage, horizontal tail, and tail location tested. All dimensions are in inches except where noted.

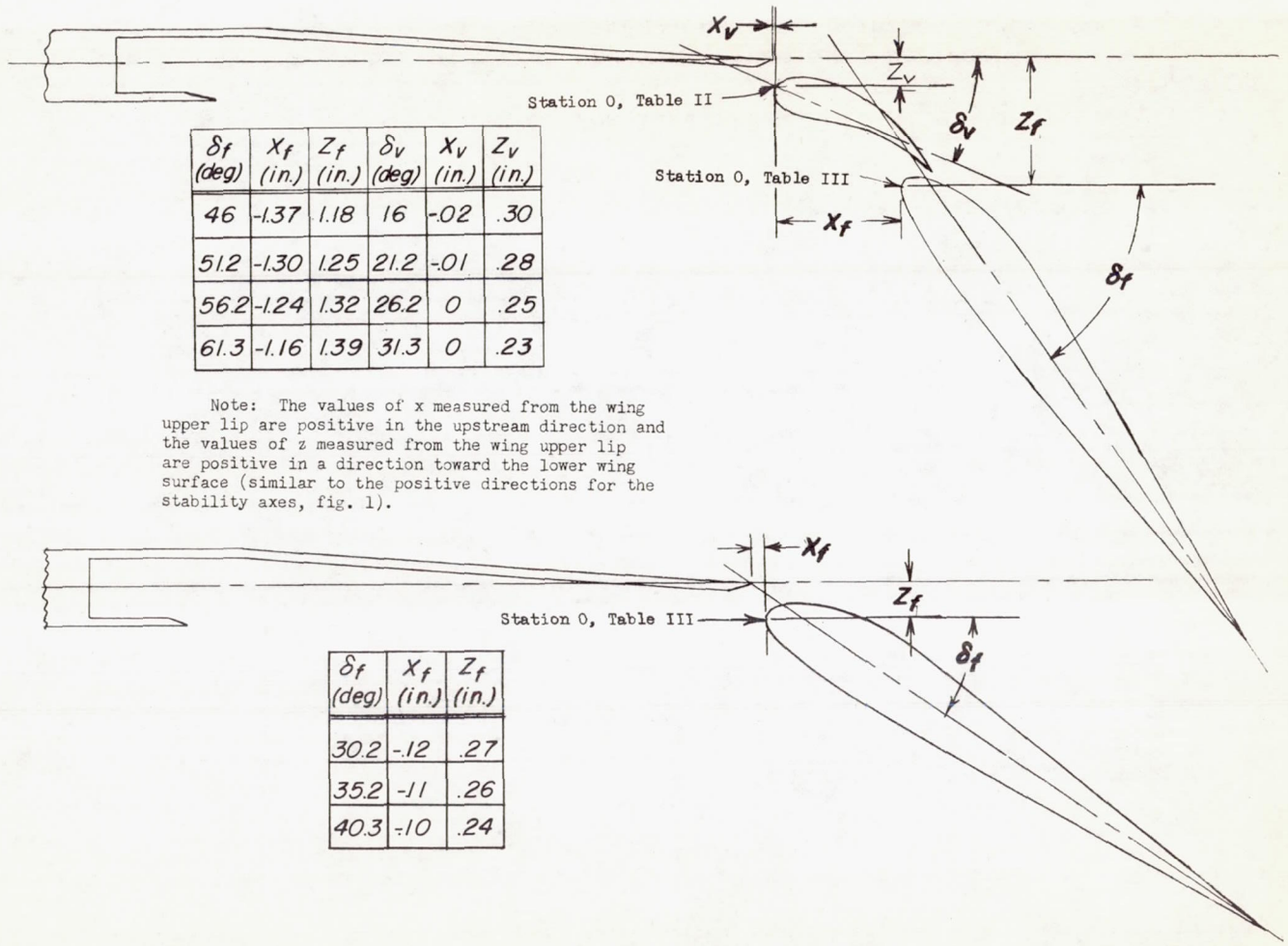

δ_f (deg)	X_f (in.)	Z_f (in.)	δ_v (deg)	X_v (in.)	Z_v (in.)
46	-1.37	1.18	16	-.02	.30
51.2	-1.30	1.25	21.2	-.01	.28
56.2	-1.24	1.32	26.2	0	.25
61.3	-1.16	1.39	31.3	0	.23

Note: The values of x measured from the wing upper lip are positive in the upstream direction and the values of z measured from the wing upper lip are positive in a direction toward the lower wing surface (similar to the positive directions for the stability axes, fig. 1).

δ_f (deg)	X_f (in.)	Z_f (in.)
30.2	-.12	.27
35.2	-.11	.26
40.3	-.10	.24

(b) Details of flaps.

Figure 2.- Continued.

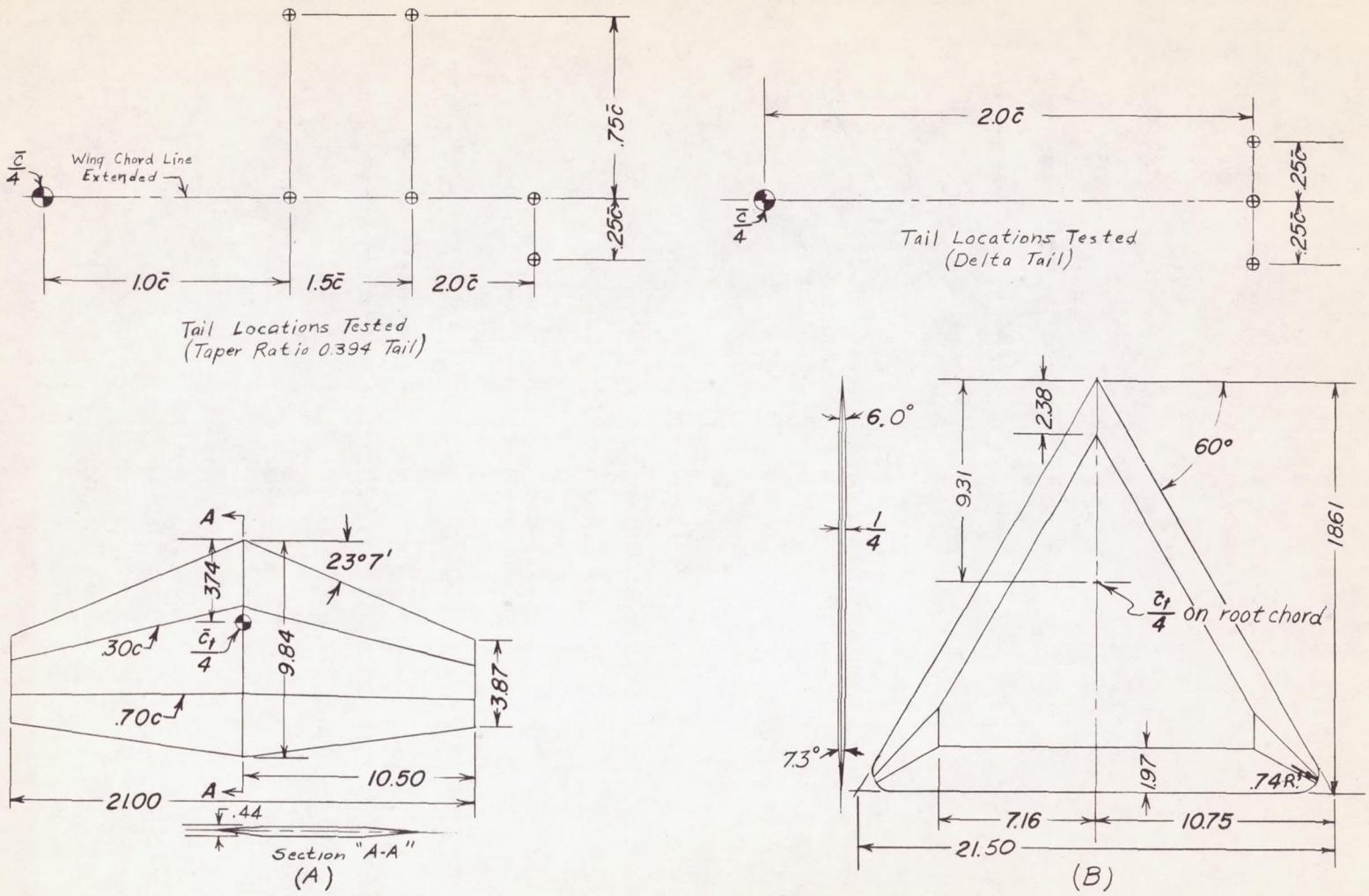

(c) Details of horizontal tails and tail locations tested.

Figure 2.- Concluded.

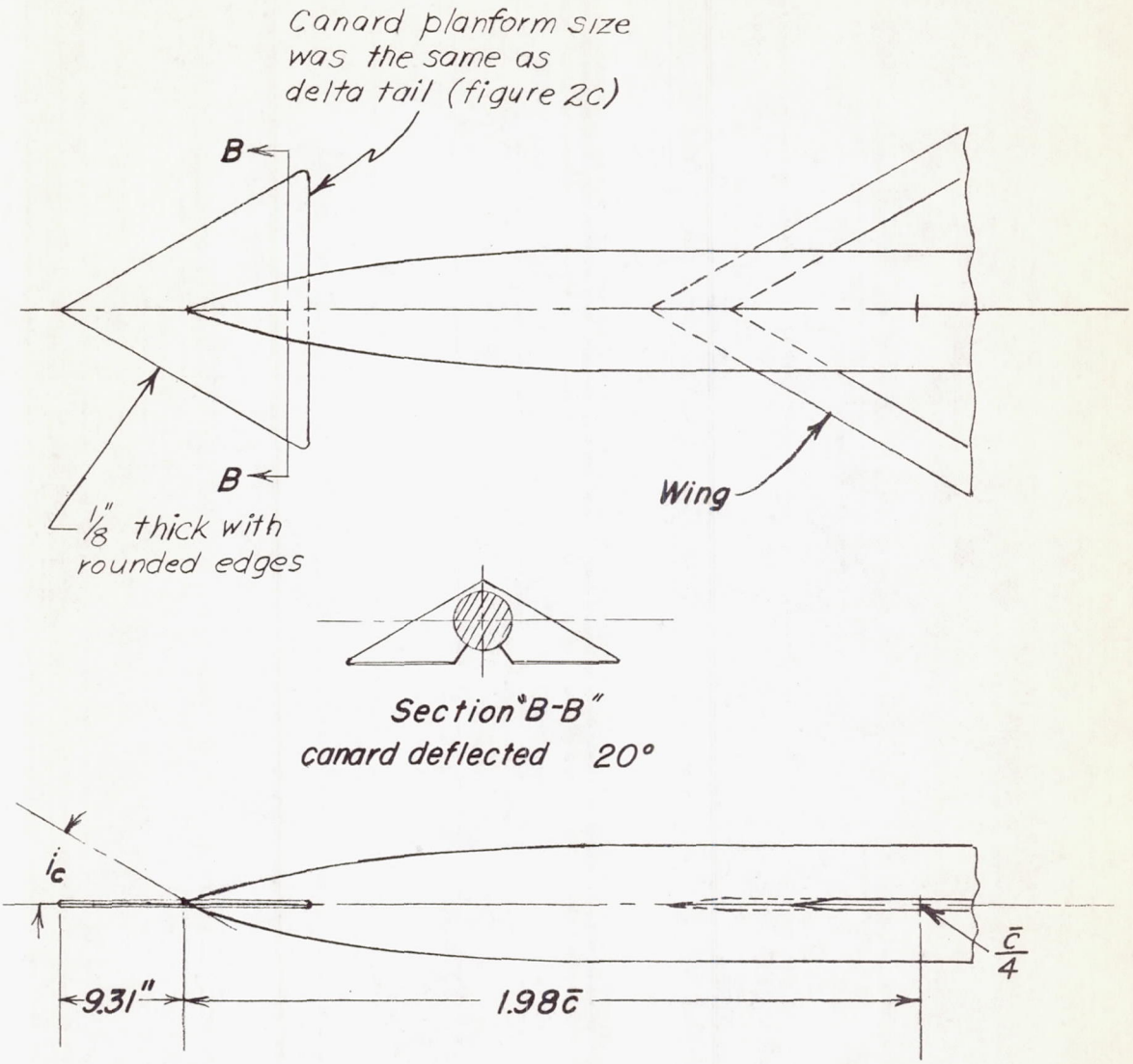

Figure 3.- Canard details.

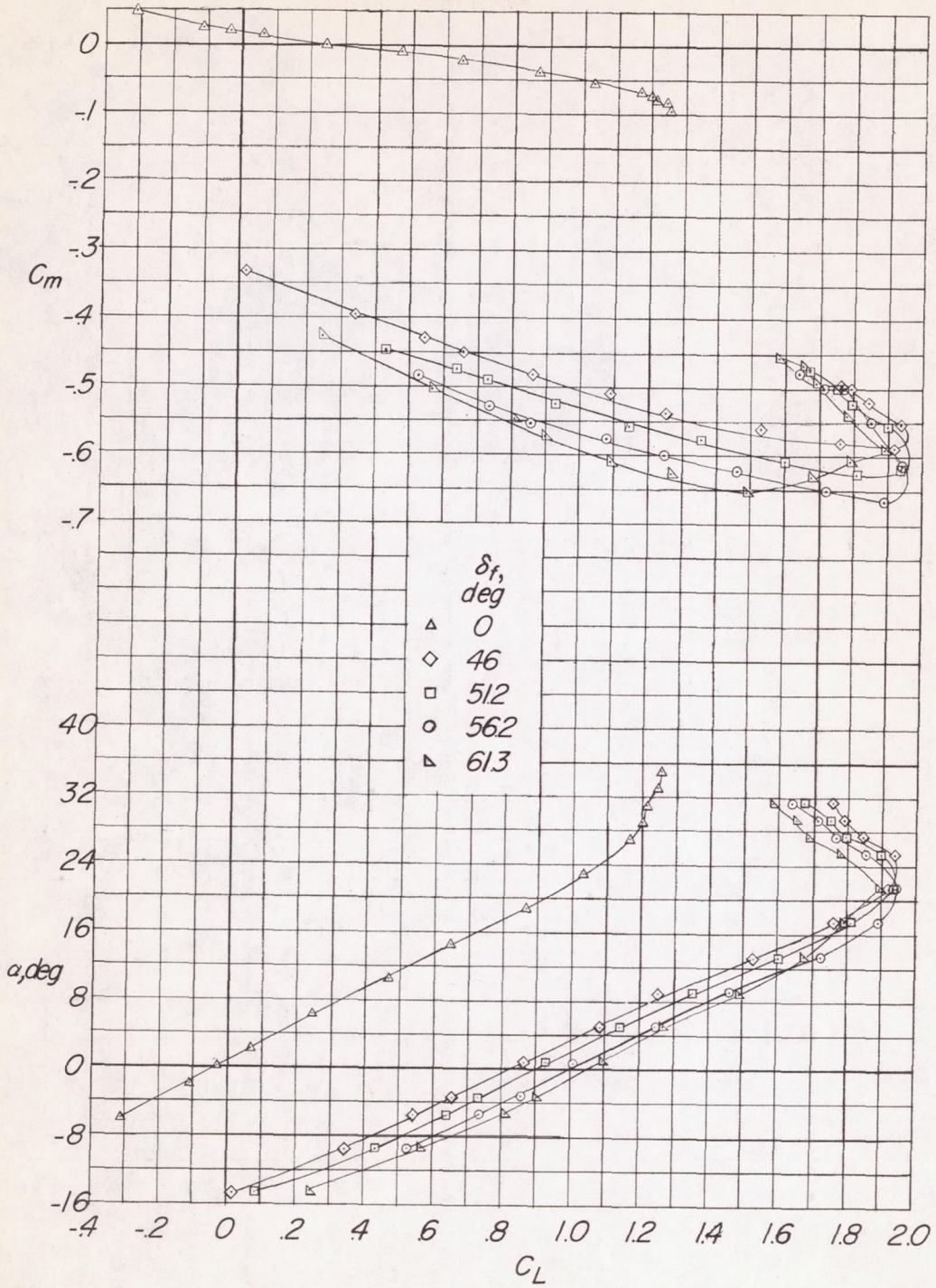

Figure 4.- Effect of deflection of the extended double slotted flaps on the longitudinal aerodynamic characteristics in pitch of the delta-wing—fuselage model. Tail off; fuselage with 1.0$\bar{c}$ afterbody. ($\delta_f = 0^o$ configuration had a 1.5$\bar{c}$ fuselage afterbody.)

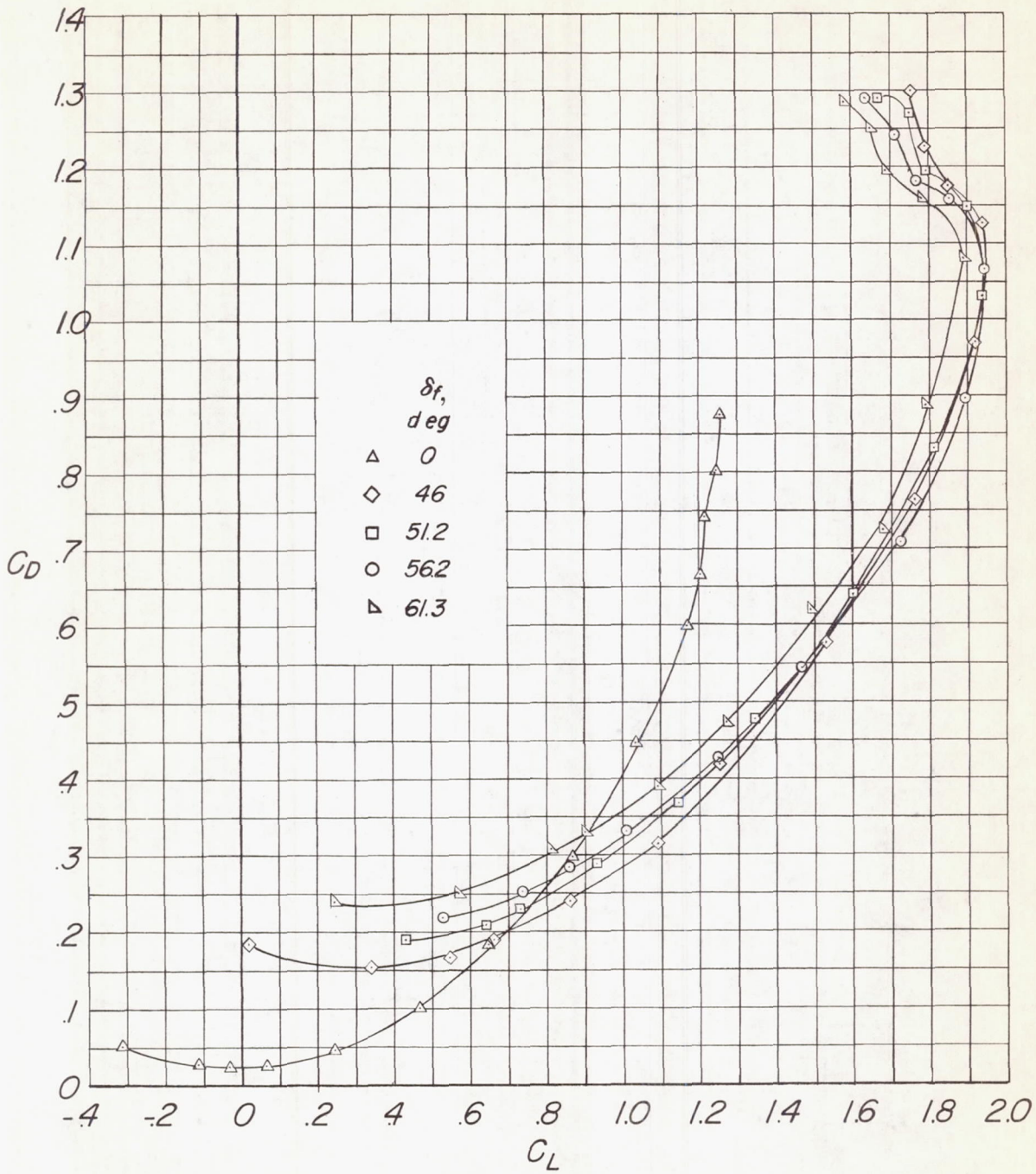

Figure 4.- Concluded.

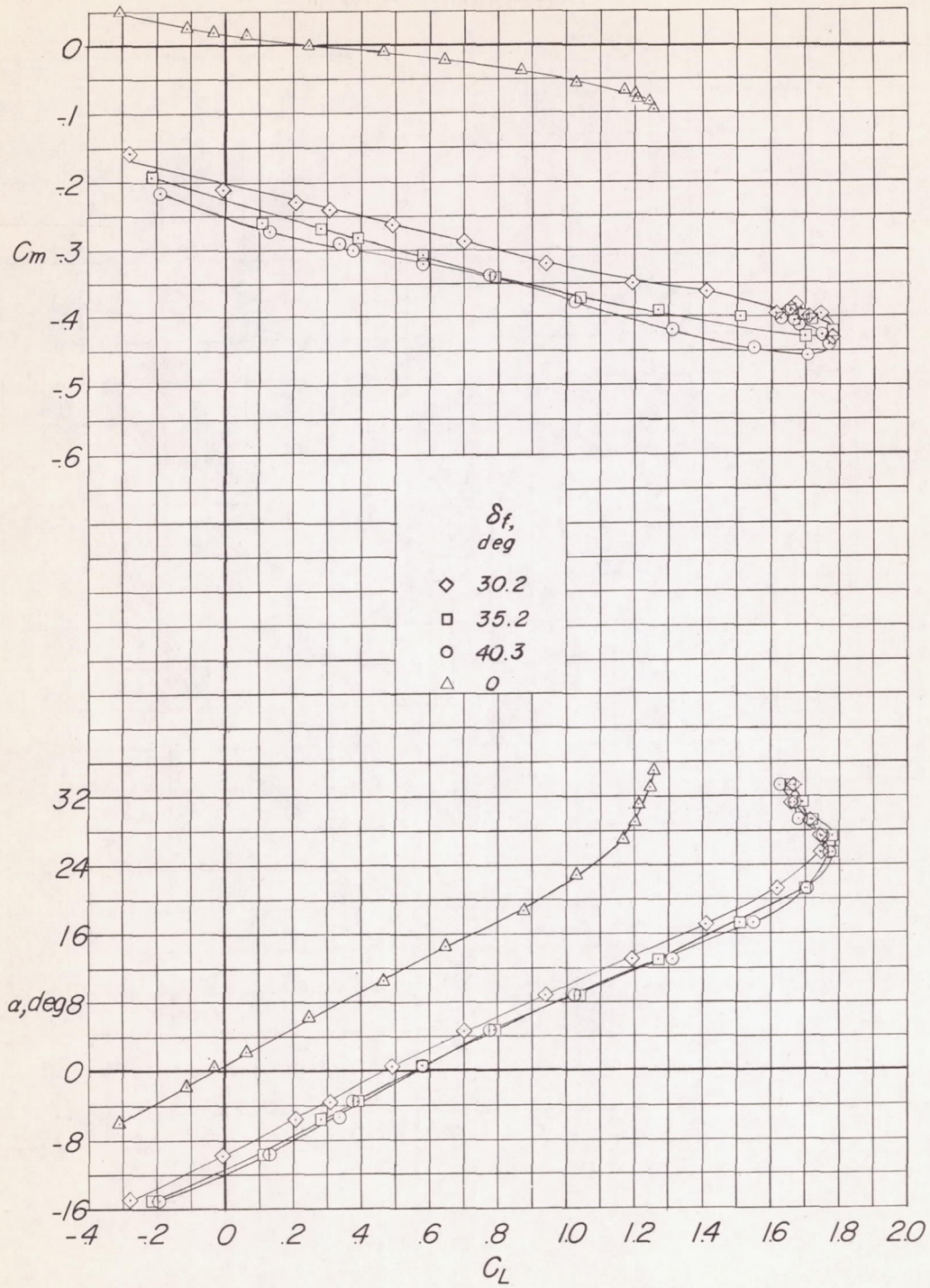

Figure 5.- Effect of deflection of an extended single slotted flap on the longitudinal aerodynamic characteristics in pitch of the delta-wing—fuselage model. Tail off; fuselage with 1.0$\bar{c}$ afterbody. ($\delta_f = 0^o$ configuration had a 1.5$\bar{c}$ fuselage afterbody.)

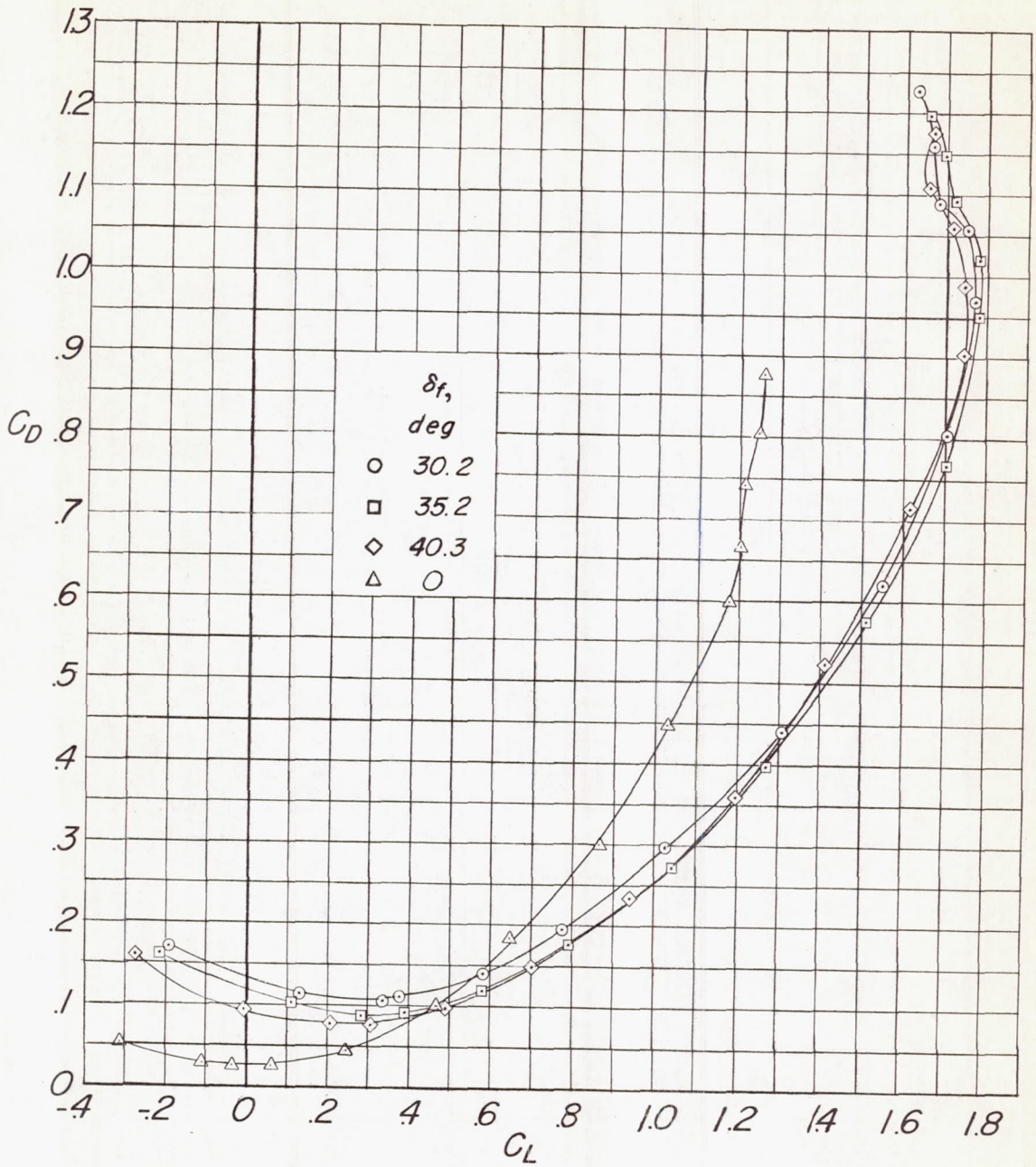

Figure 5.- Concluded.

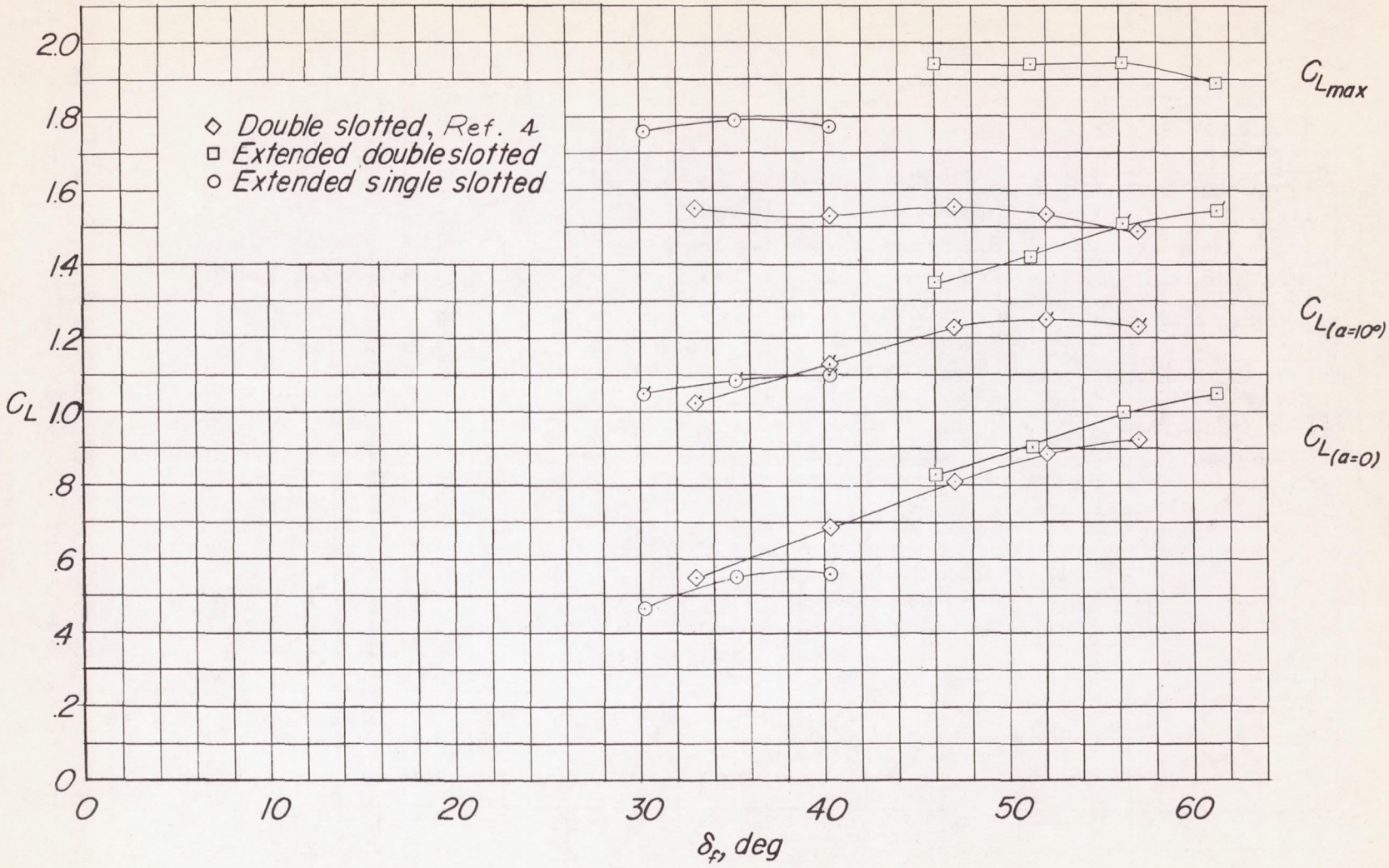

Figure 6.- The variation of C_L with flap deflection for various flaps at $\alpha = 0^\circ$, 10°, and $C_{L_{max}}$.

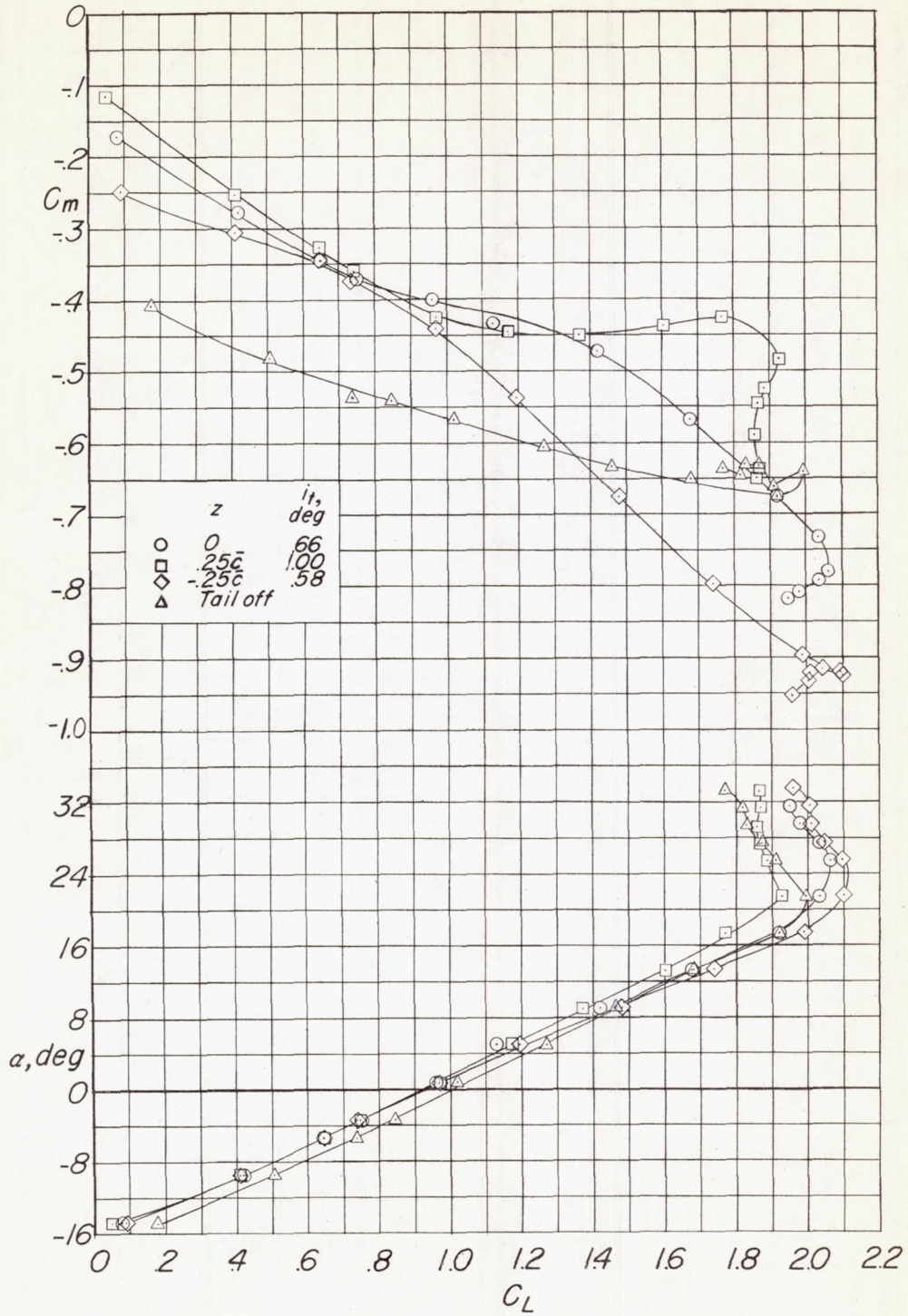

Figure 7.- Effect of location of the delta horizontal tail on the longitudinal aerodynamic characteristics in pitch of the delta-wing—fuselage model with extended double slotted flaps deflected 56.2°. $l = 2.0\bar{c}$.

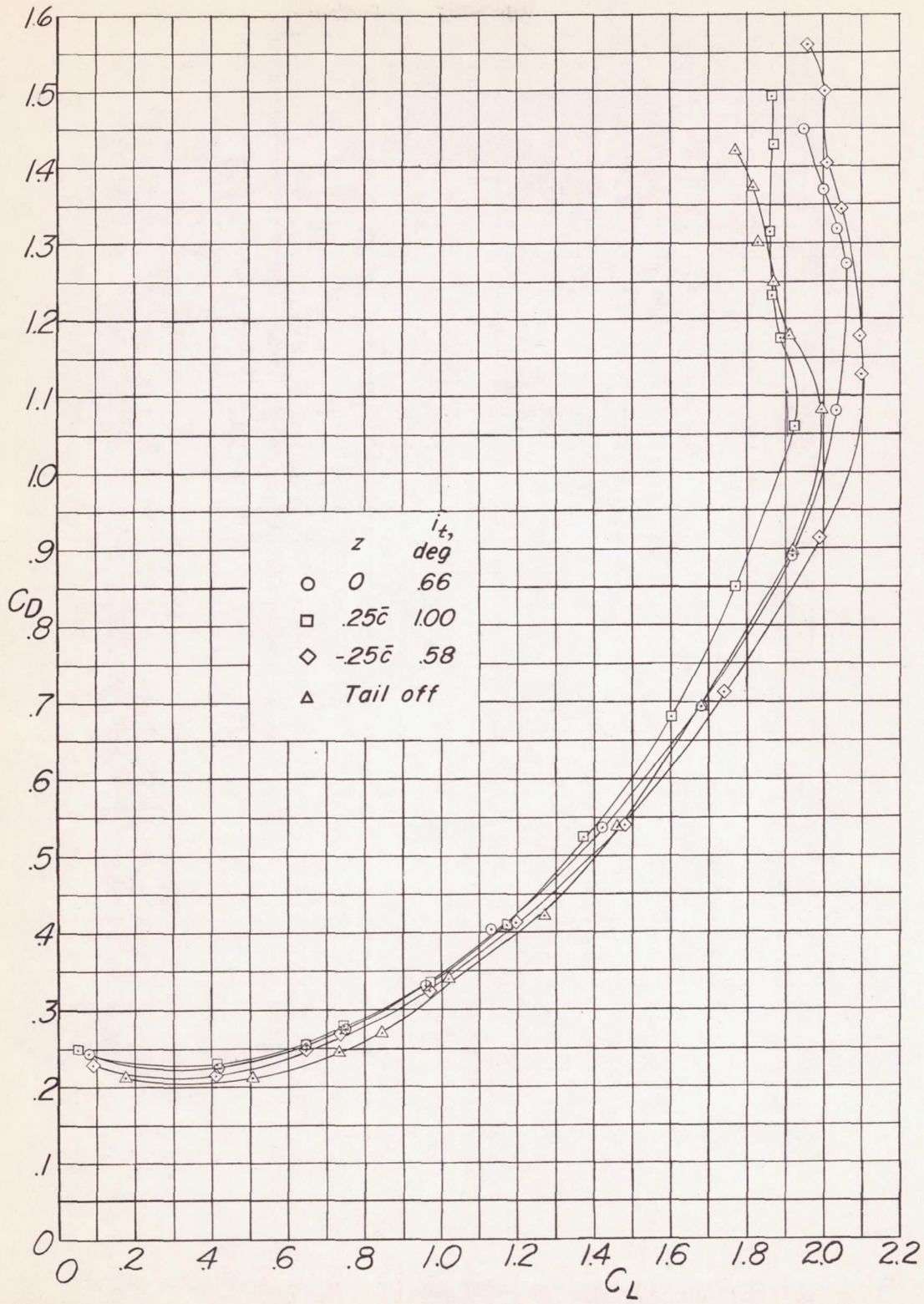

Figure 7.- Concluded.

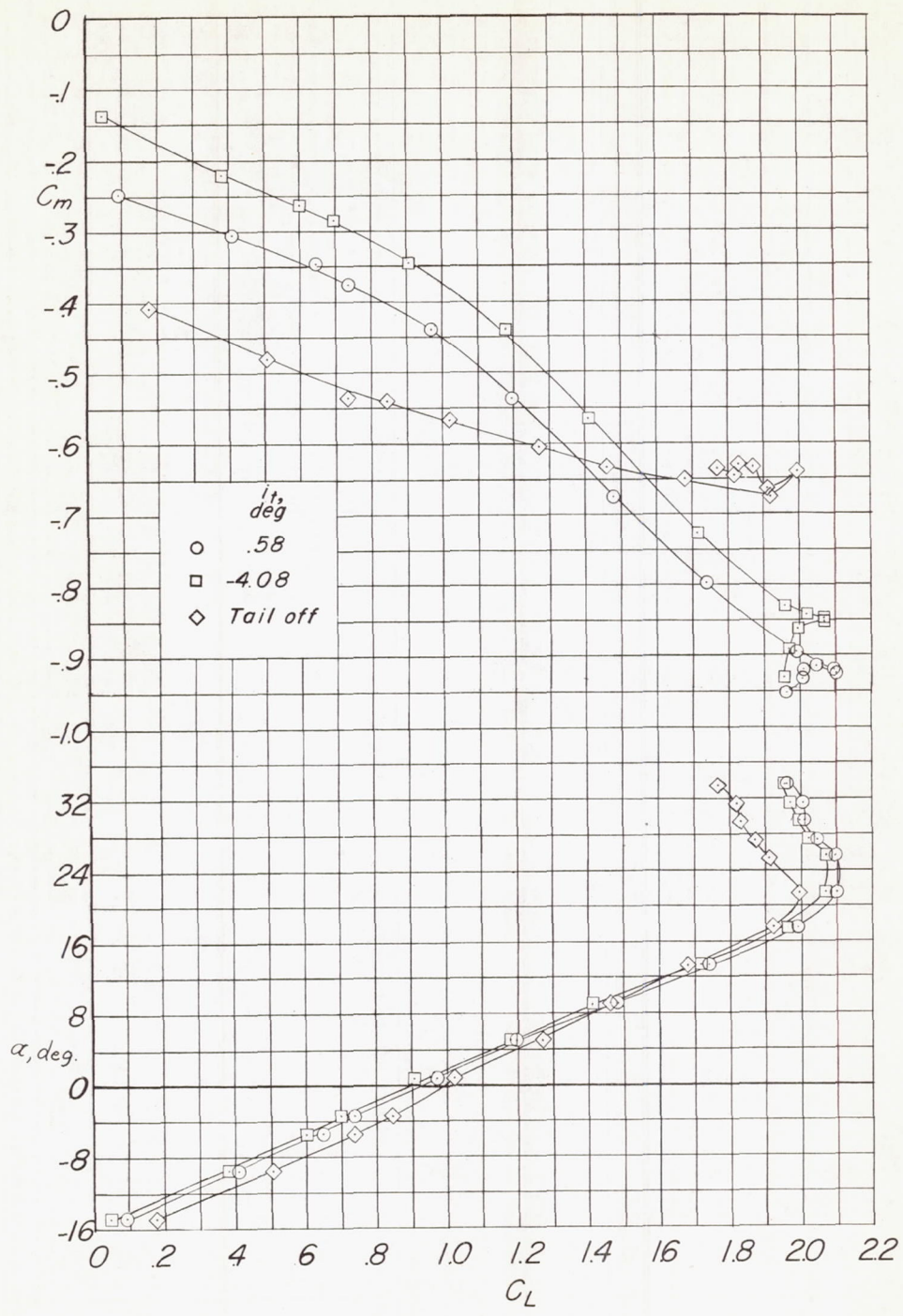

(a) $l = 2.0\bar{c}$; $z = -0.25\bar{c}$.

Figure 8.- Effect of incidence of the delta horizontal tail on the longitudinal aerodynamic characteristics in pitch of the delta-wing—fuselage model with extended double slotted flaps at 56.2°.

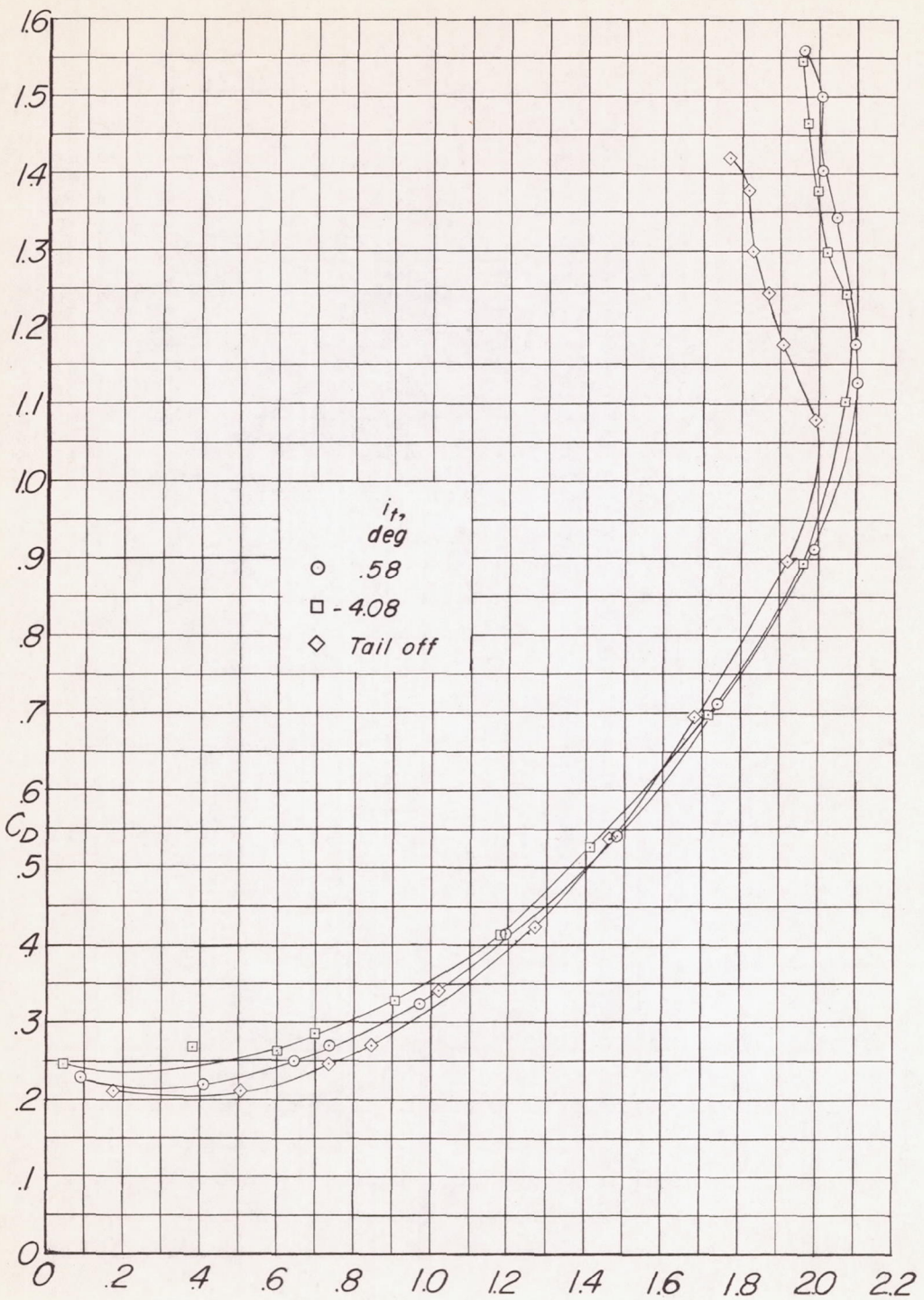

(a) Concluded.

Figure 8.- Continued.

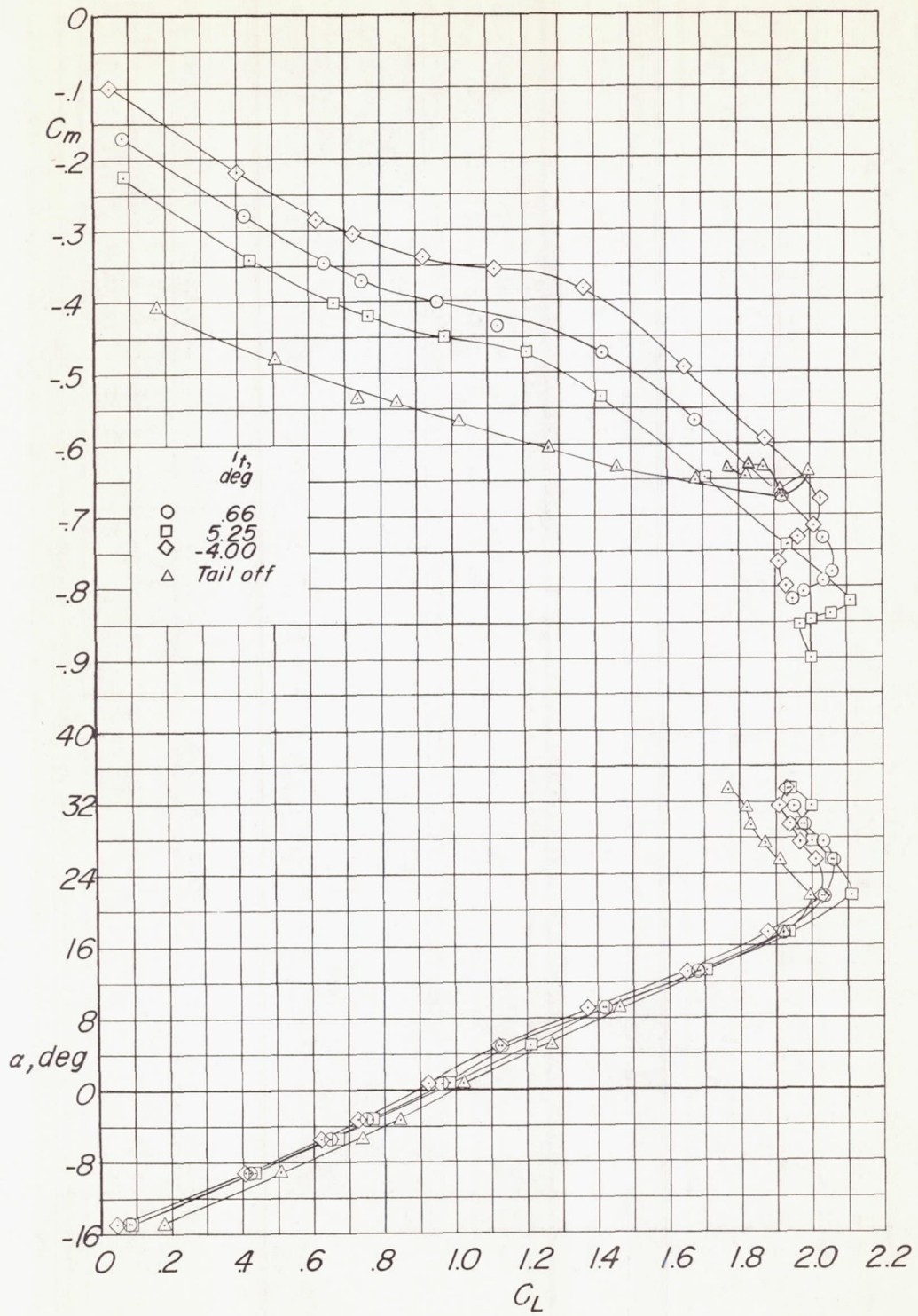

(b) $l = 2.0\bar{c}$; $z = 0$.

Figure 8.- Continued.

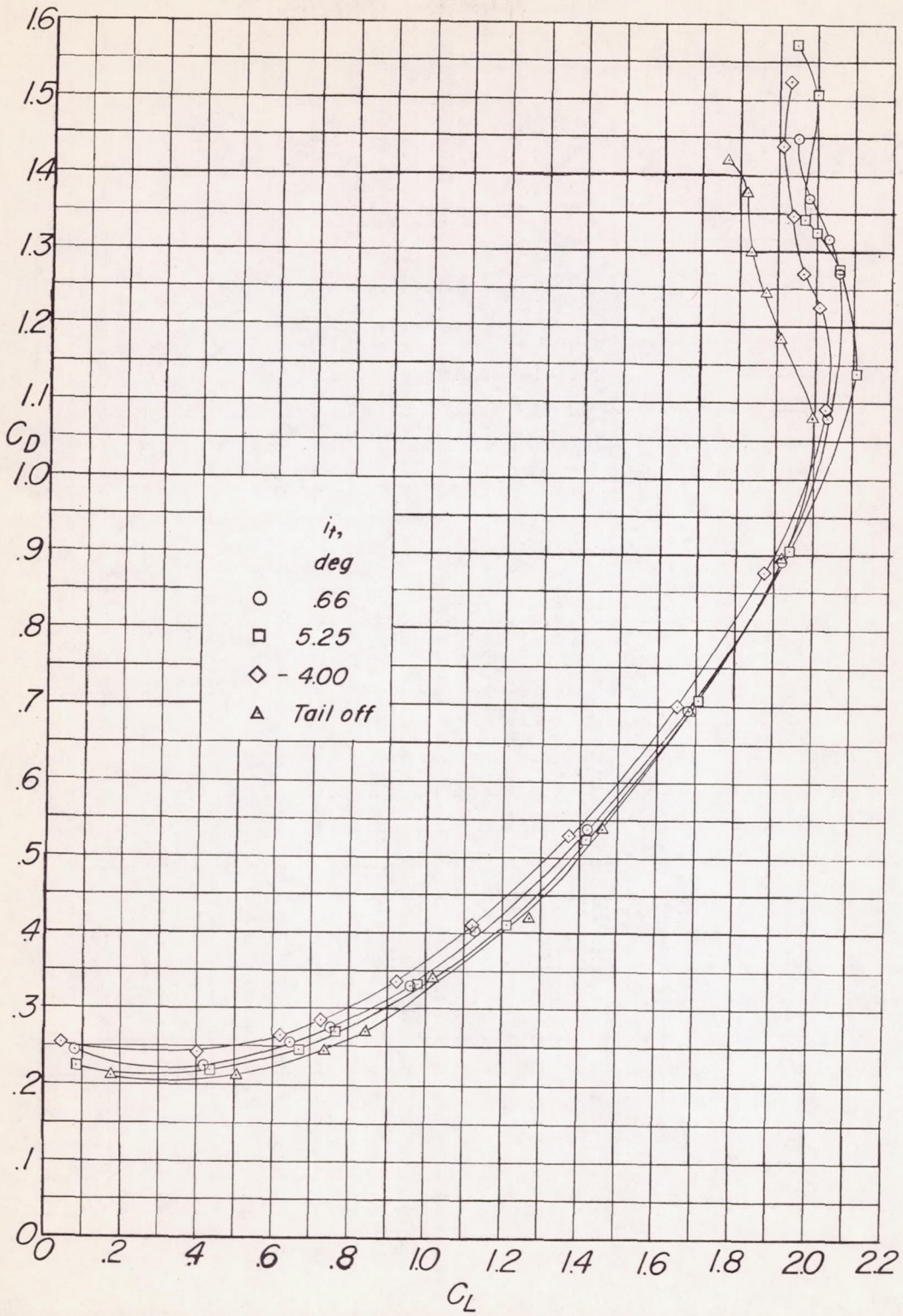

(b) Concluded.

Figure 8.- Concluded.

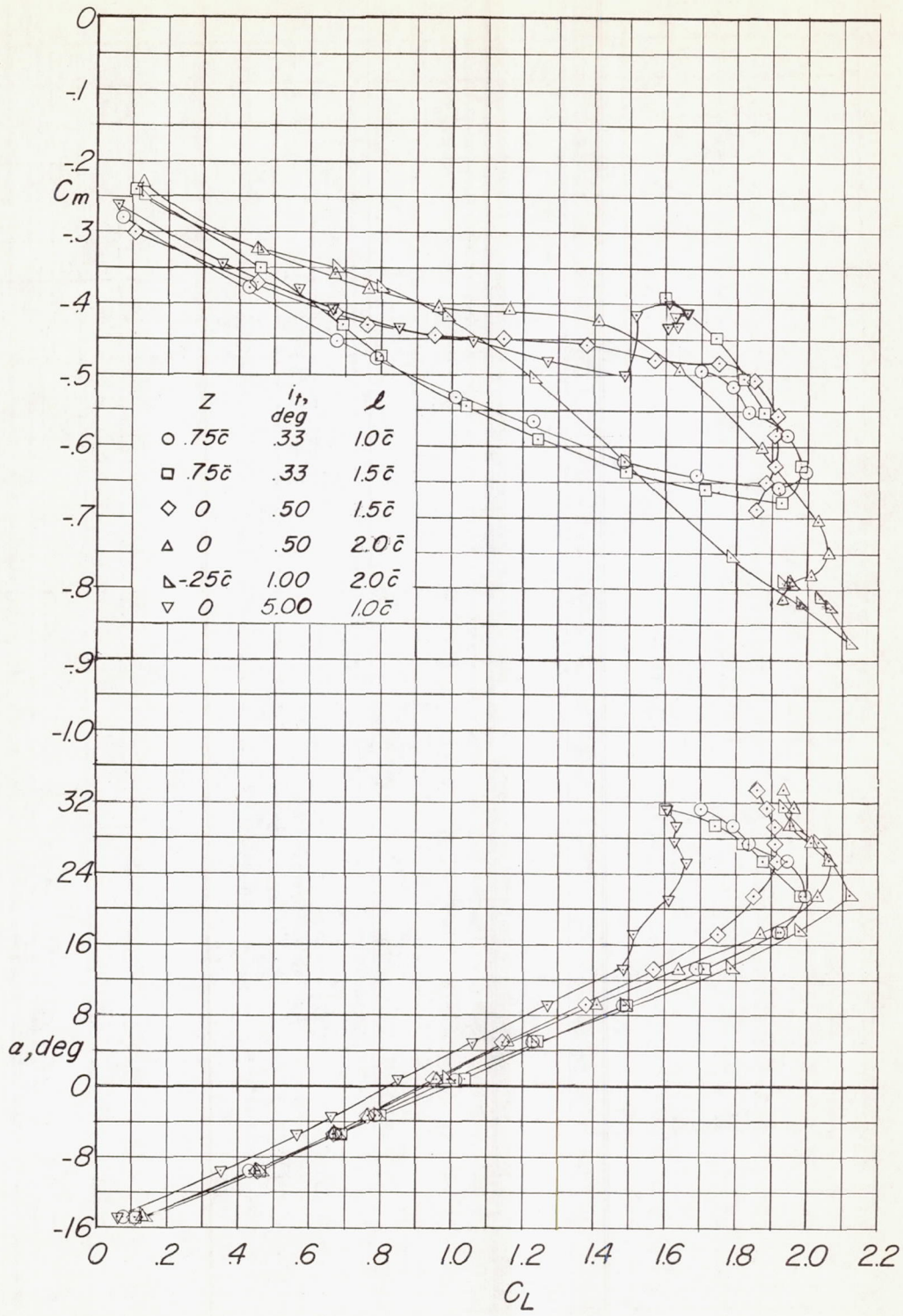

Figure 9.- Effect of location of the tail with a taper ratio of 0.394 on the longitudinal aerodynamic characteristics in pitch of the delta-wing—fuselage model with extended double slotted flaps at 56.2°.

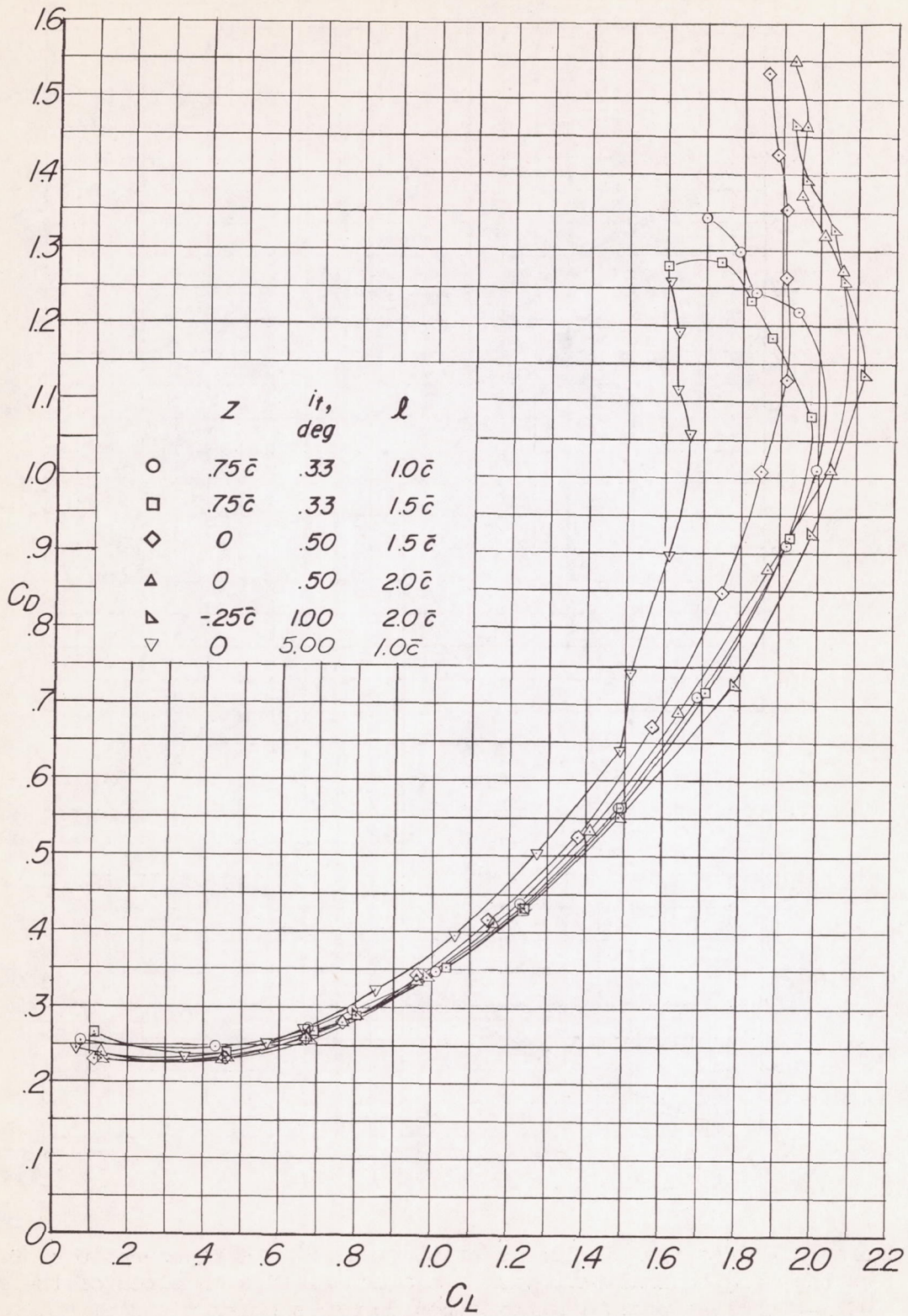

Figure 9.- Concluded.

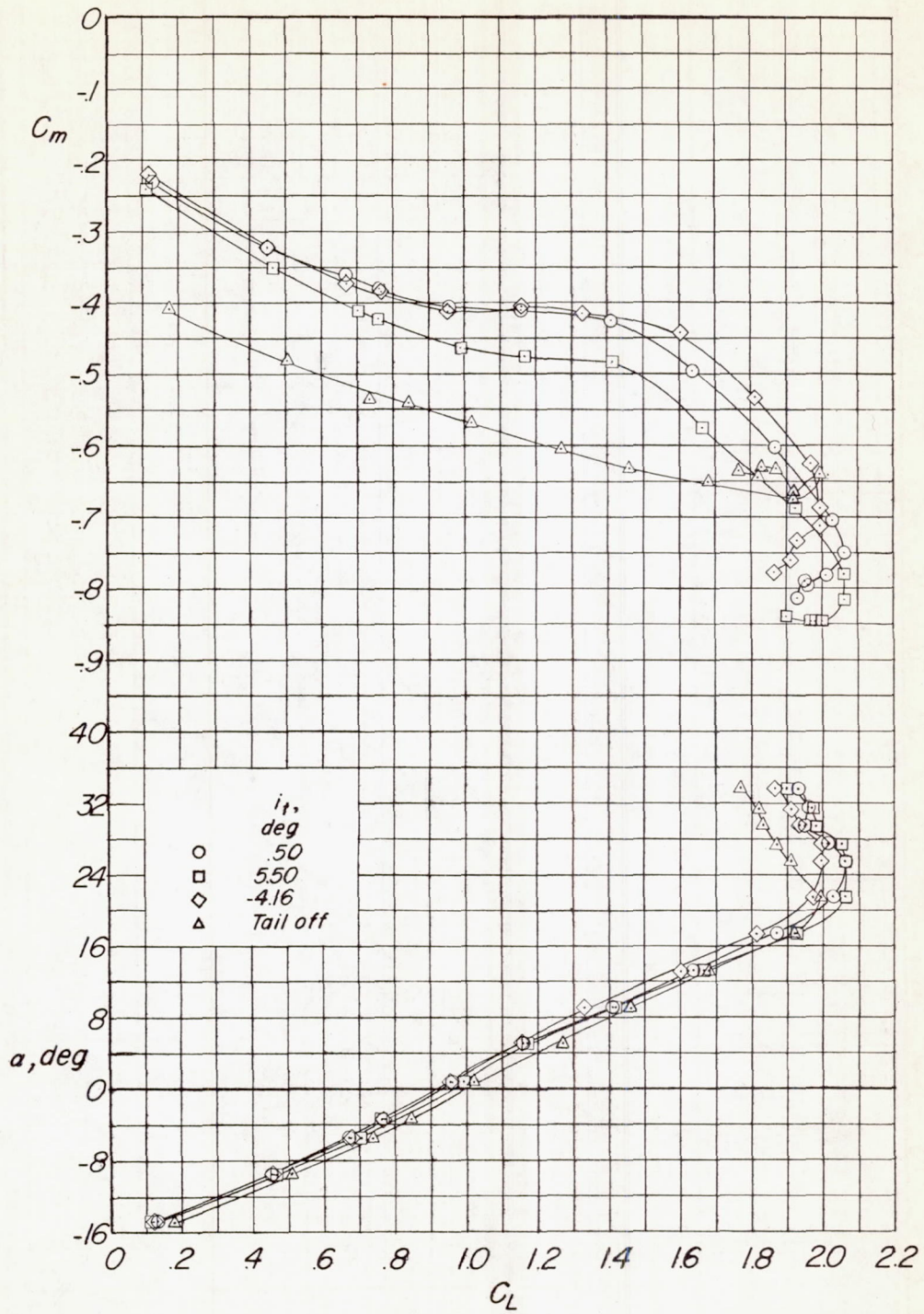

Figure 10.- Effect of incidence of the tail with a taper ratio of 0.394 on the longitudinal aerodynamic characteristics in pitch of the delta-wing—fuselage model with extended double slotted flaps at 56.2° deflection. $z = 0$; $l = 2.0\bar{c}$.

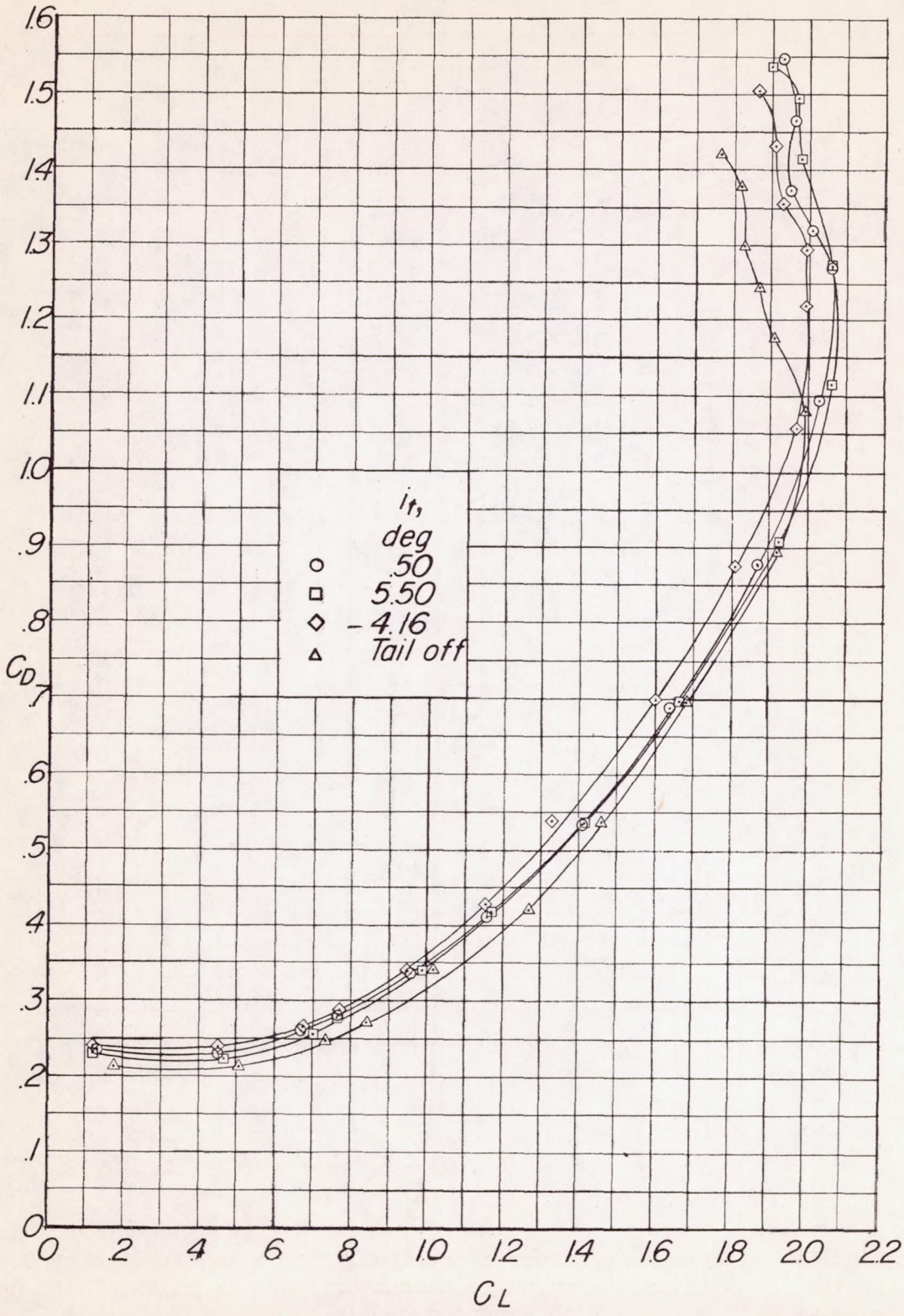

Figure 10.- Concluded.

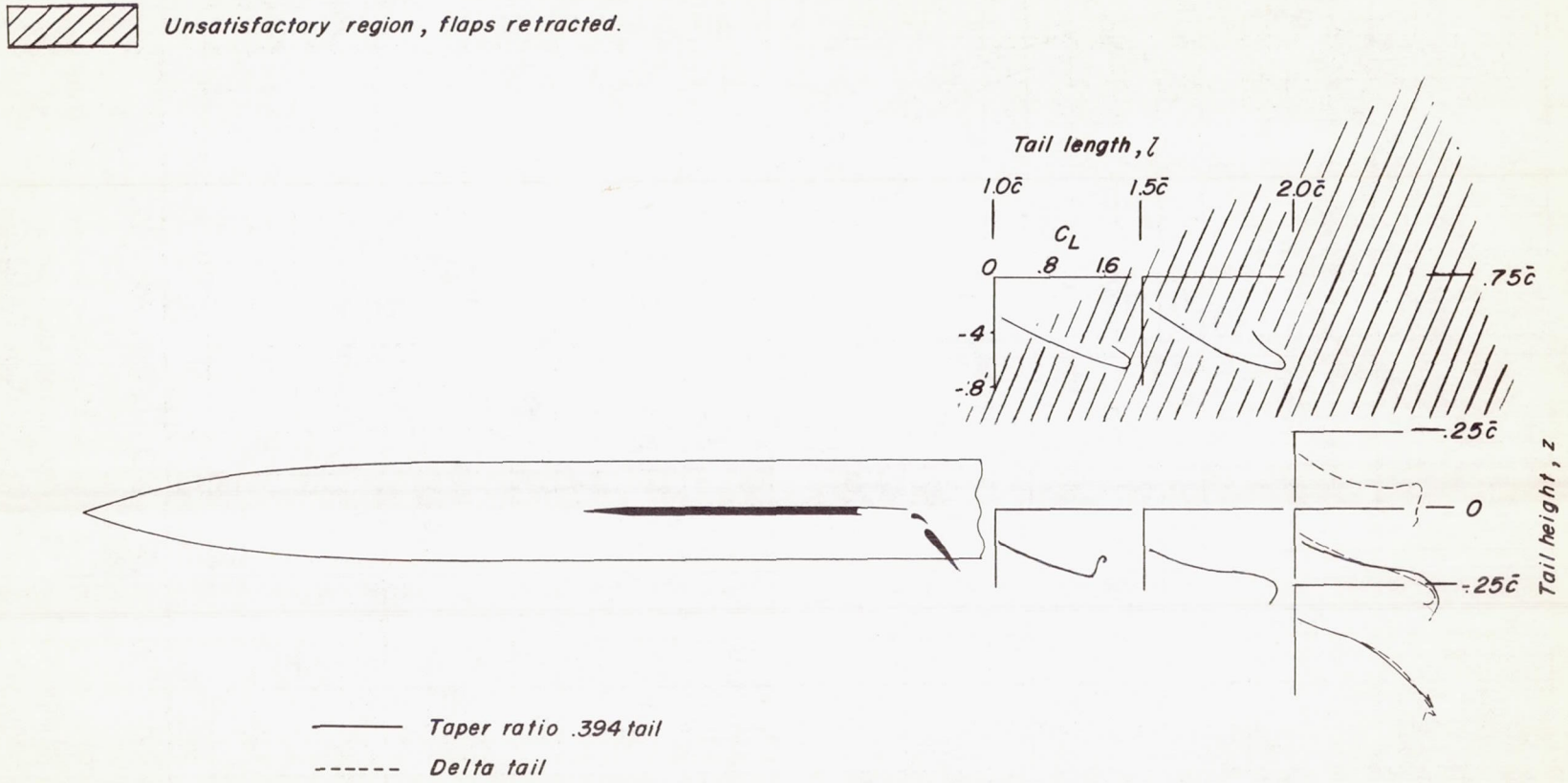

Figure 11.- Summary of the effect of the two horizontal tails on the curve of C_M against C_L of the model with extended double slotted flaps deflected 56.2°.

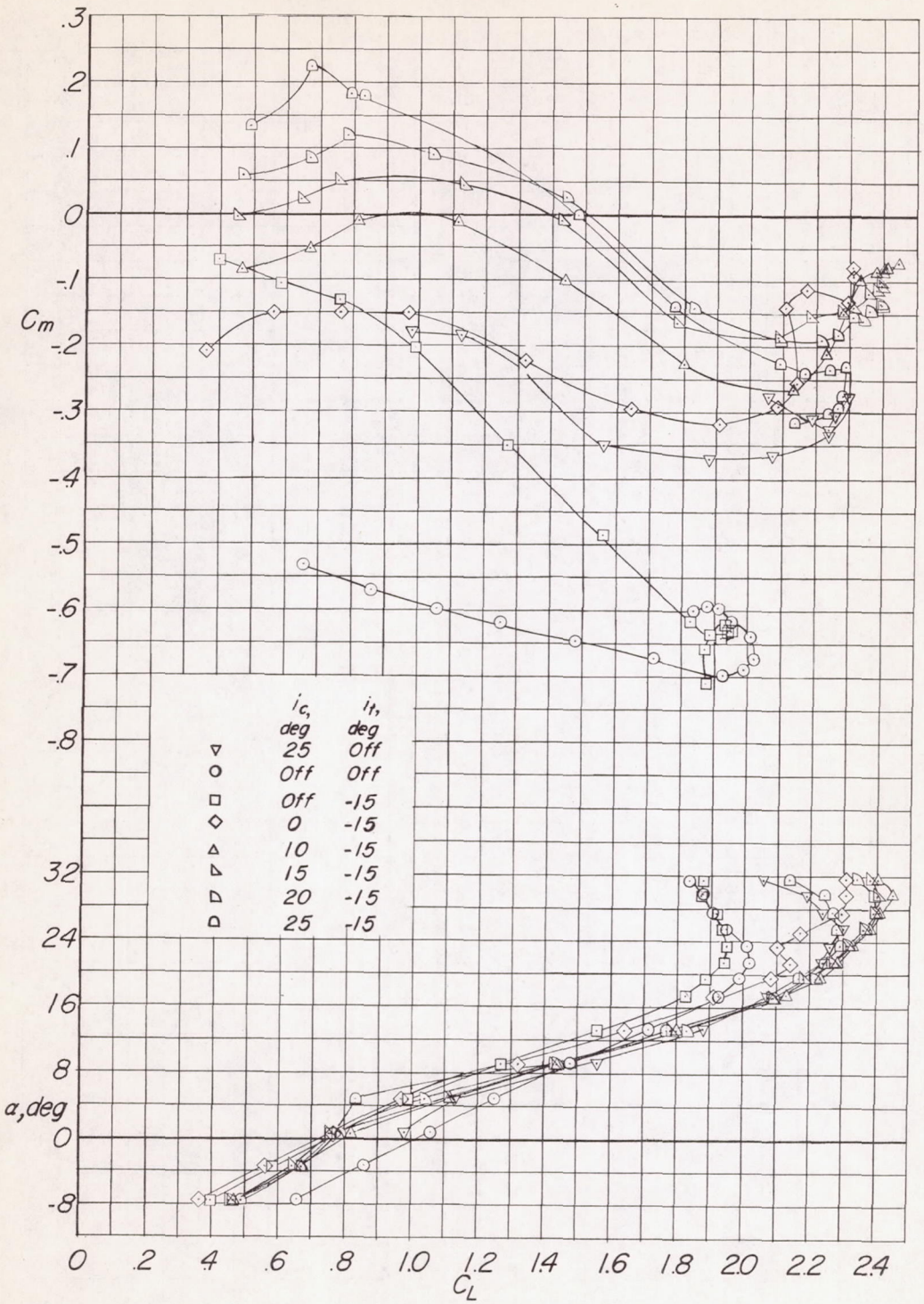

Figure 12.- Effect of incidence of canard on the longitudinal aerodynamic characteristics in pitch of the delta-wing—fuselage model with delta tail and extended double slotted flaps deflected 56.2°. $l = 2.0\bar{c}$ and $z = -0.25\bar{c}$.

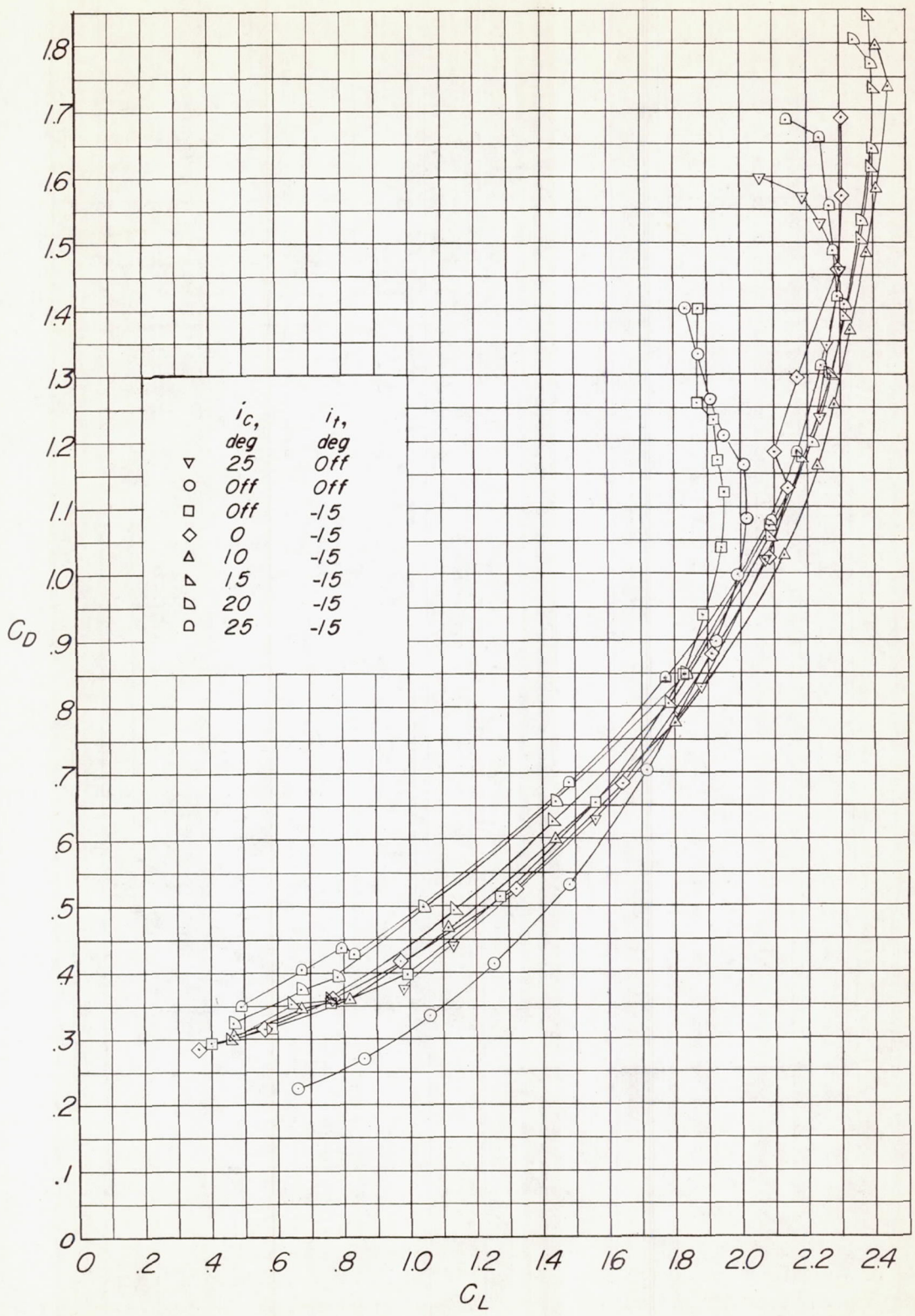

Figure 12.- Concluded.

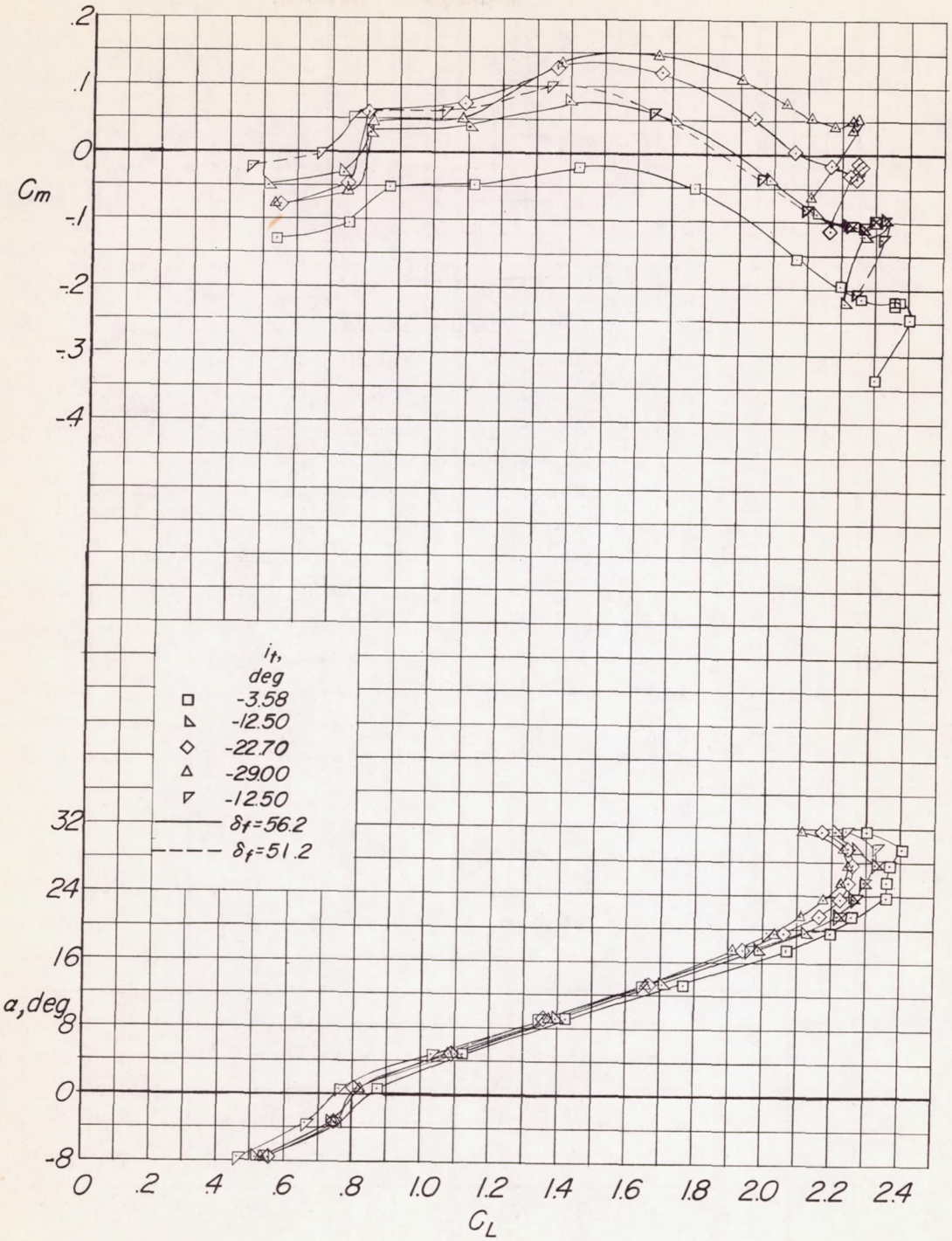

(a) $i_c = 20^\circ$; $z = 0$.

Figure 13.- Effect of delta-tail incidence with canard on the longitudinal aerodynamic characteristics in pitch of the delta-wing—fuselage model with extended double slotted flaps. $l = 2.0\bar{c}$.

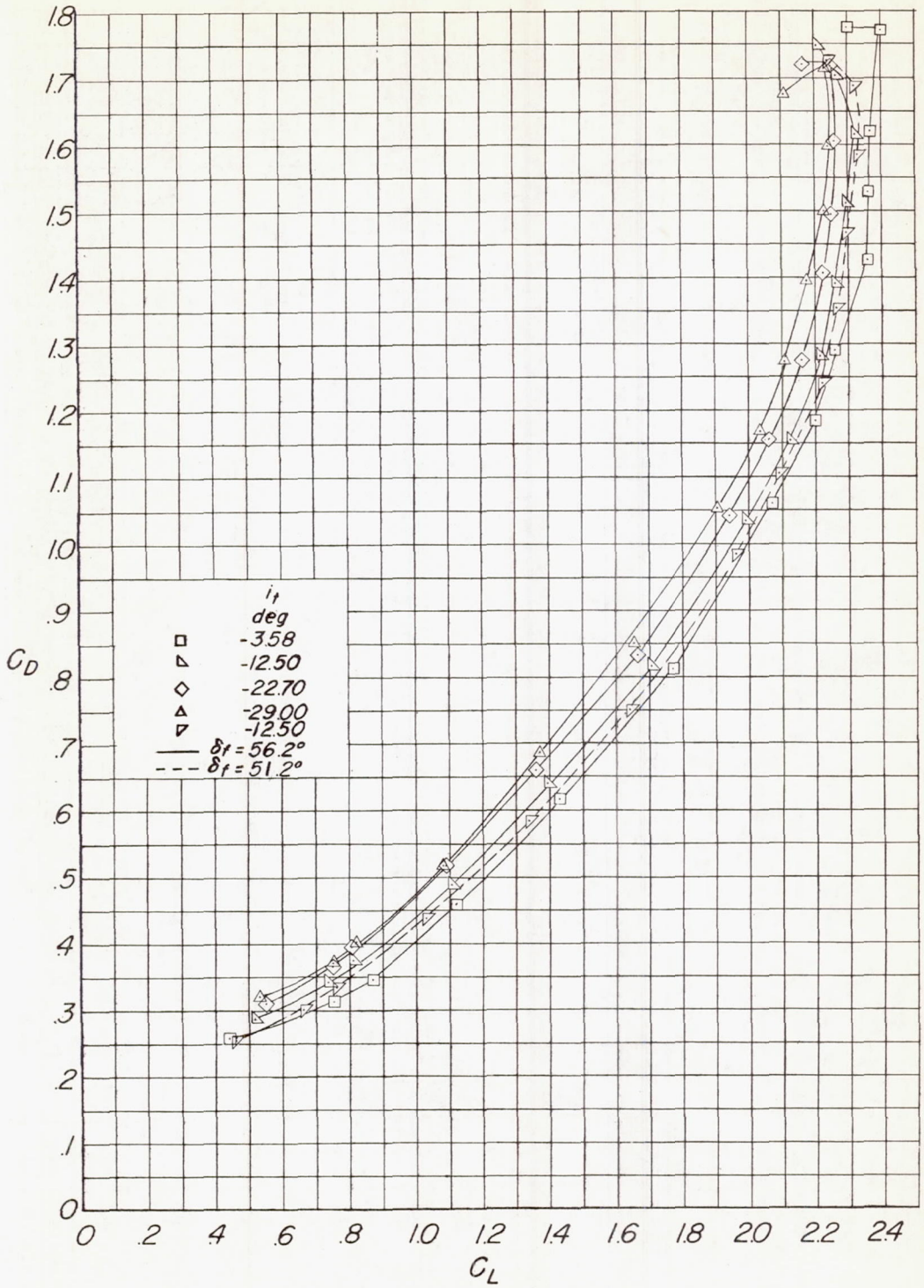

(a) Concluded.

Figure 13.- Continued.

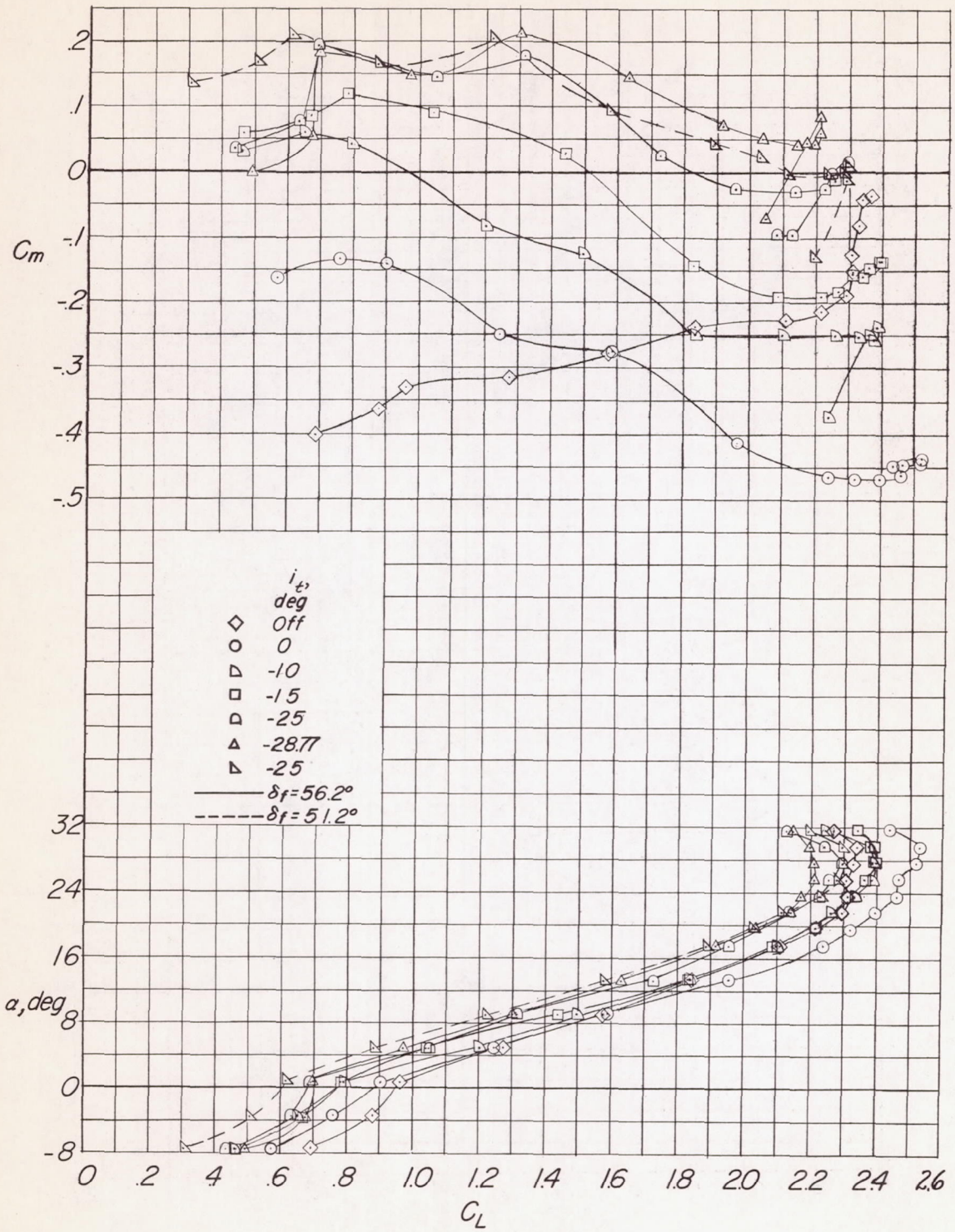

(b) $i_c = 20^\circ$; $z = -0.25\bar{c}$.

Figure 13.- Continued.

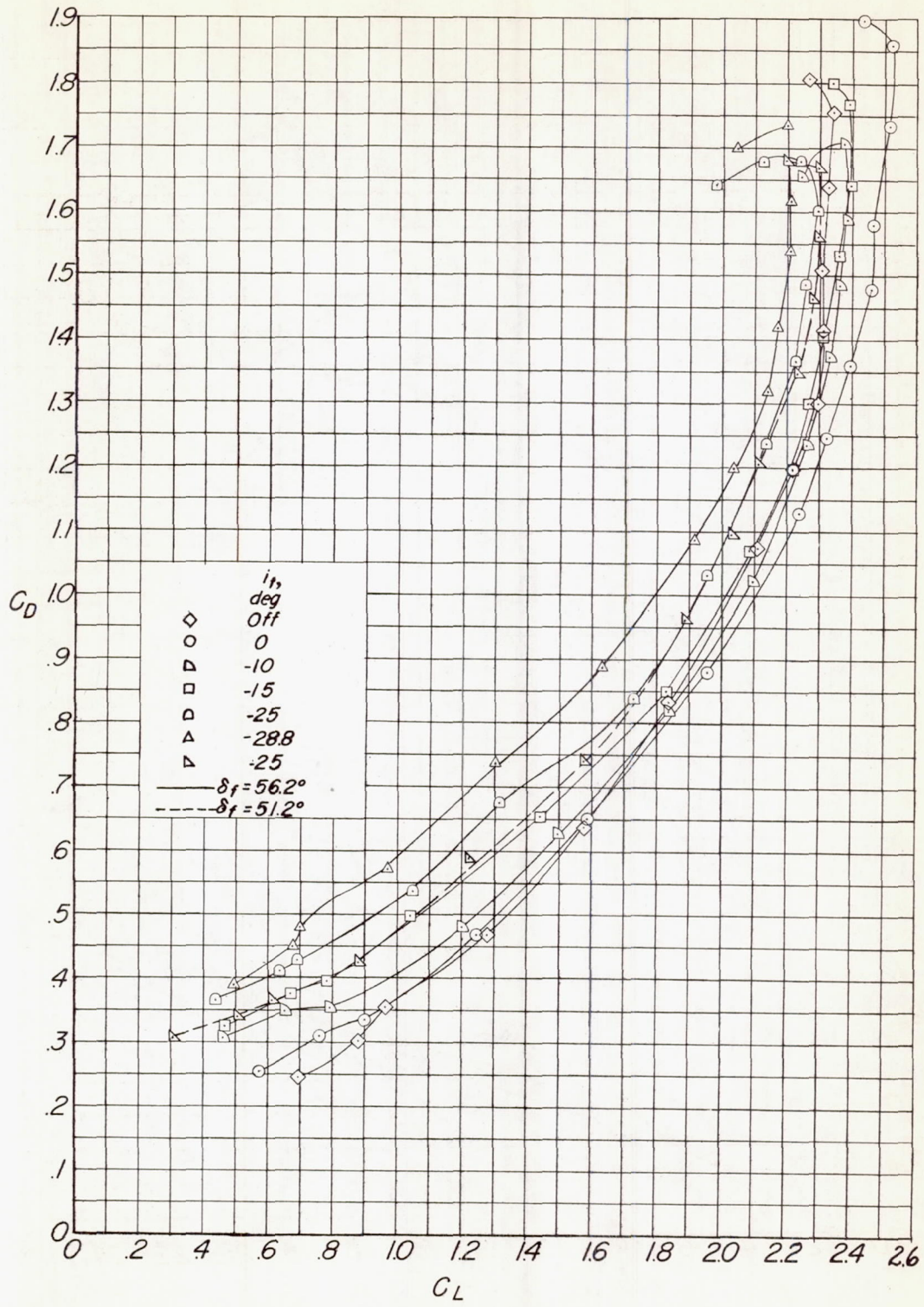

(b) Concluded.

Figure 13.- Continued.

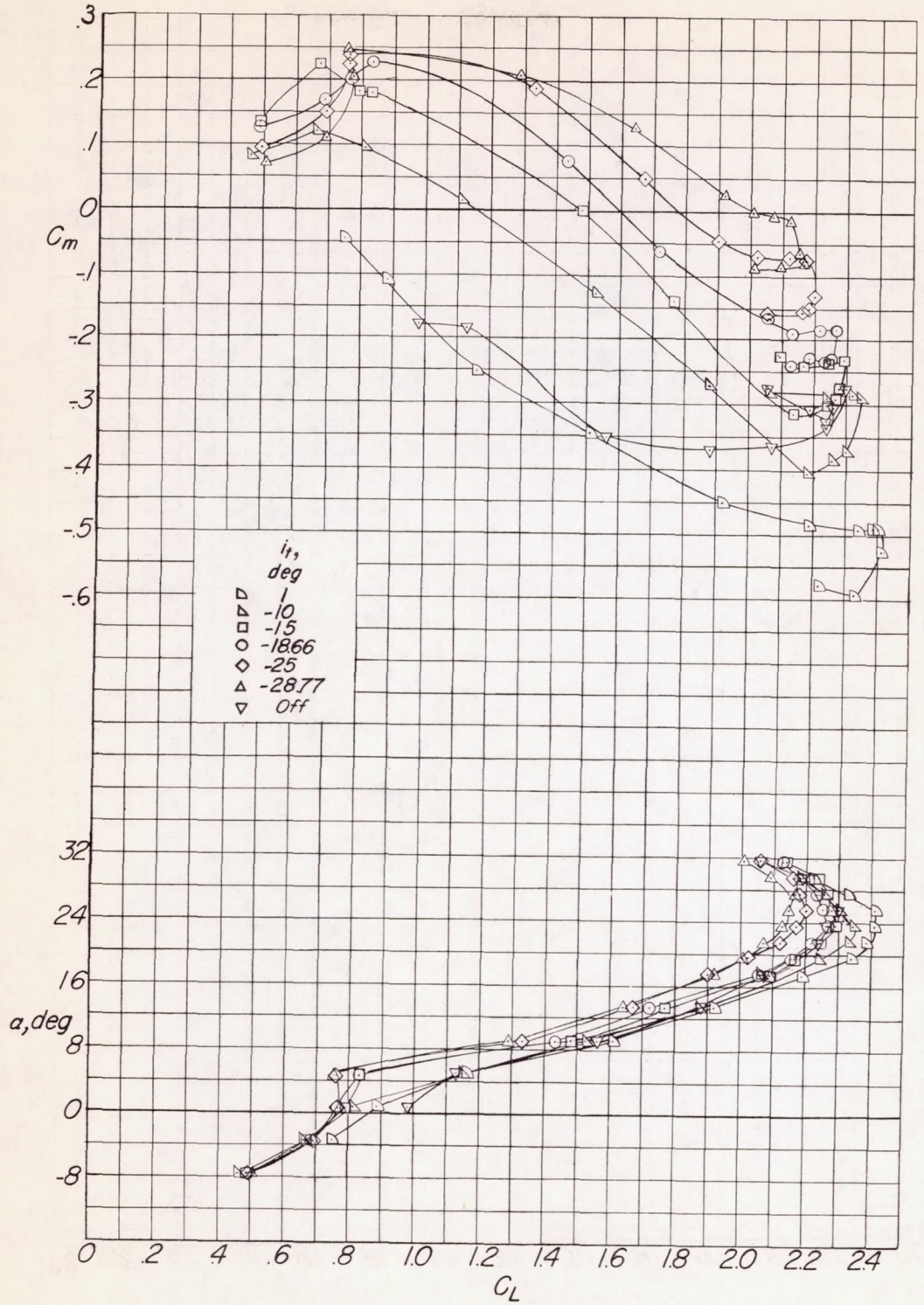

(c) $i_c = 25^\circ$; $z = -0.25\bar{c}$.

Figure 13.- Continued.

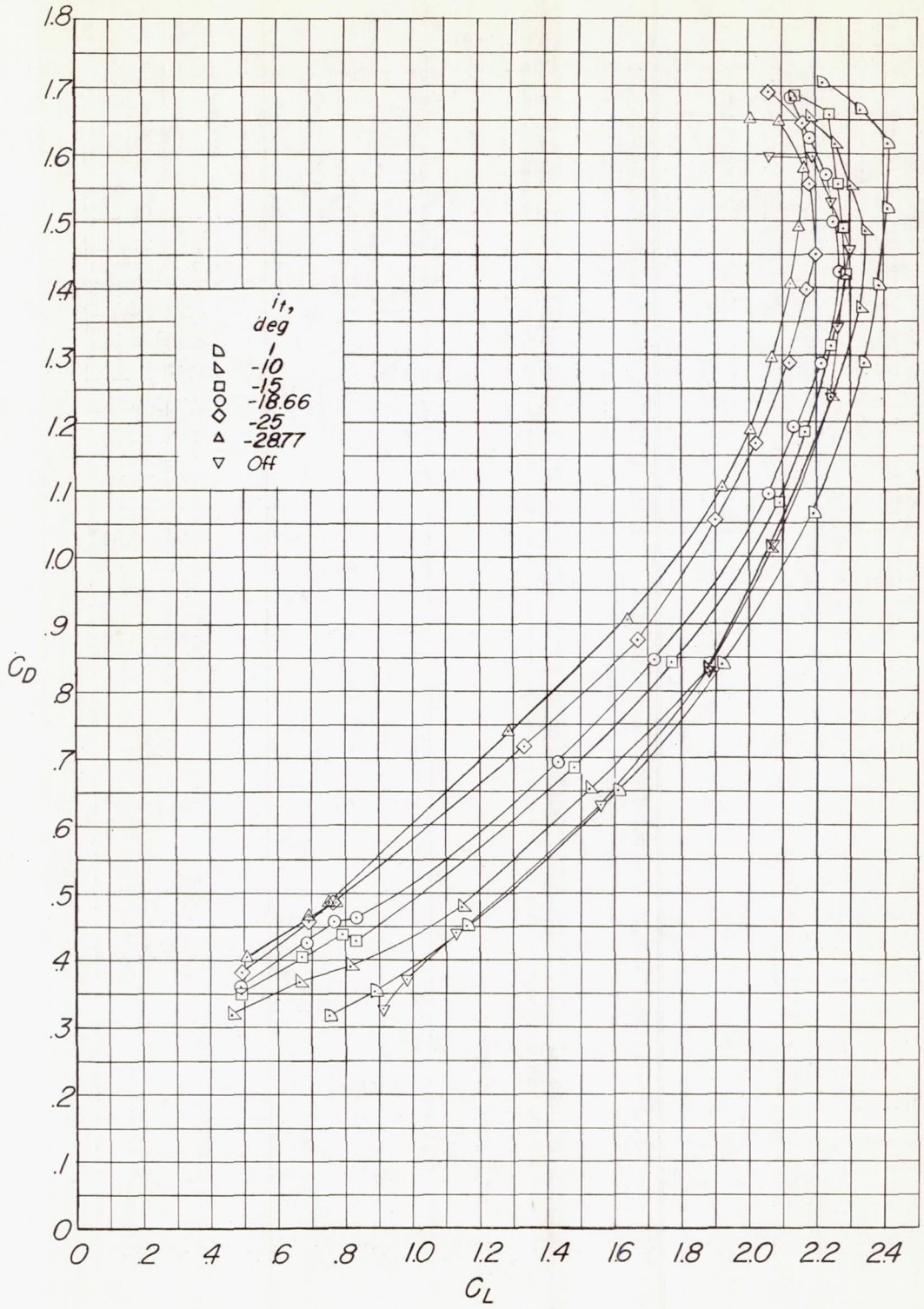

(c) Concluded.

Figure 13.- Concluded.

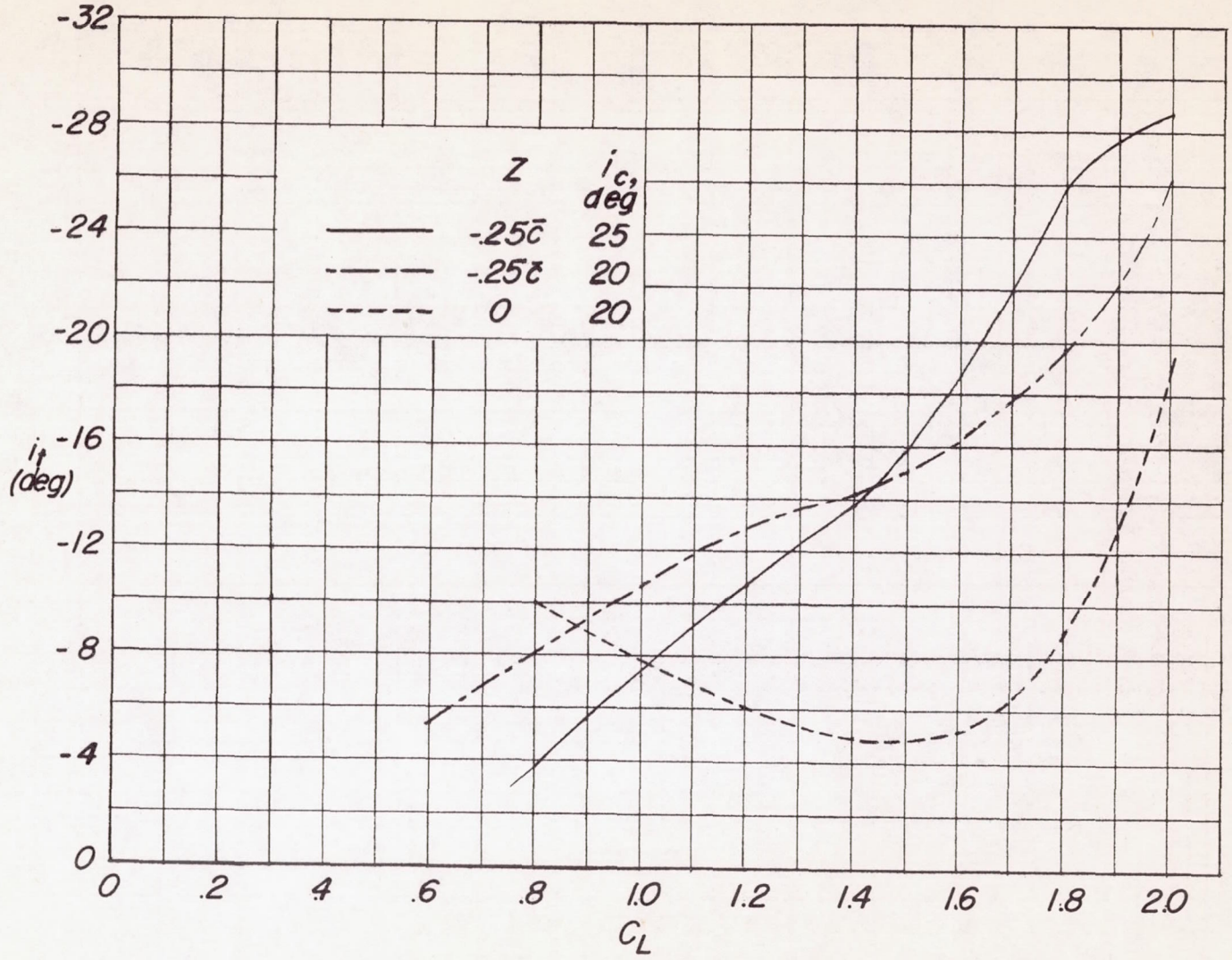

Figure 14.- Estimated delta-tail incidence required for trim at $l = 2.0\bar{c}$. Extended double slotted flap deflection 56.2°.

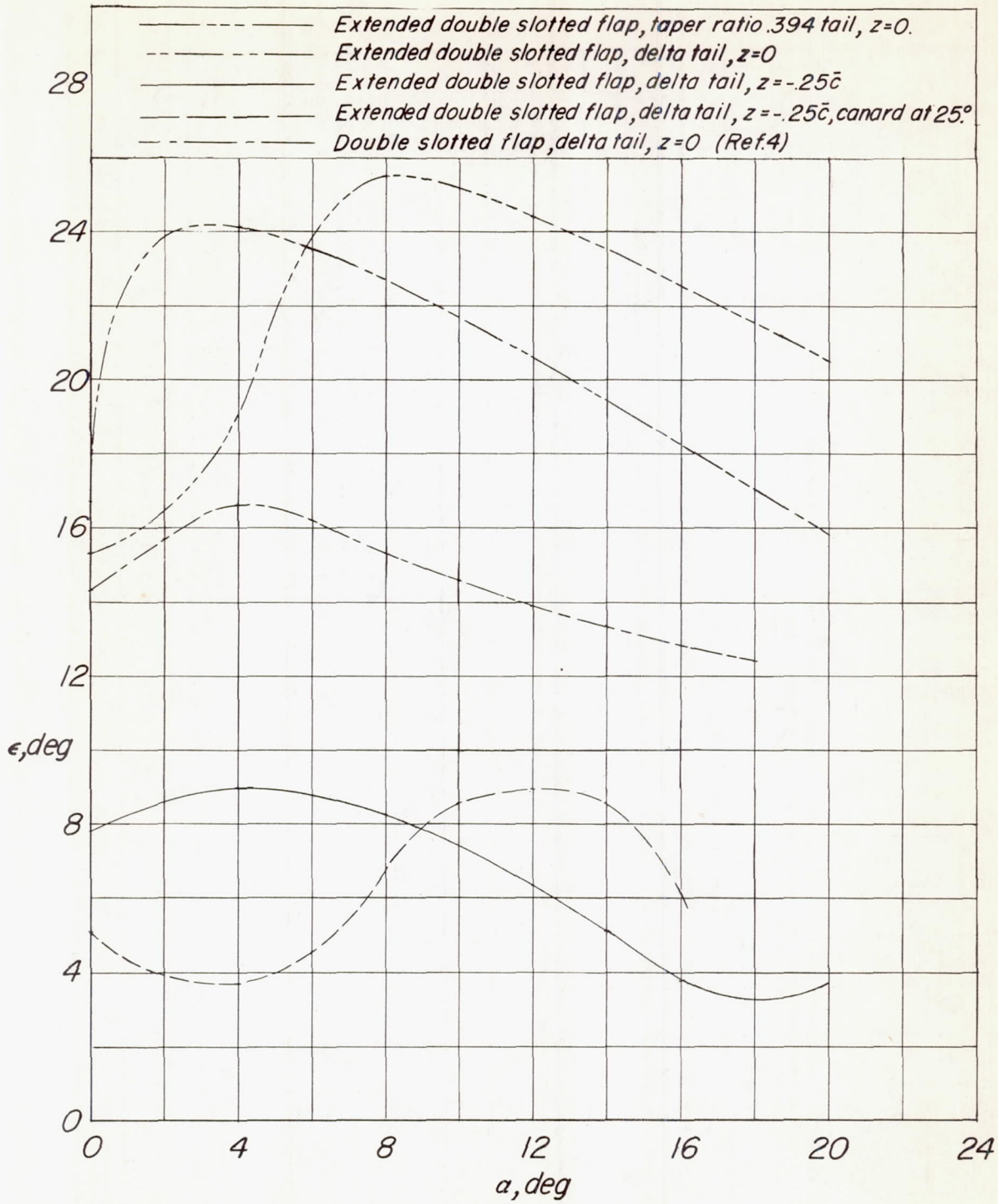

Figure 15.- Variation of the effective downwash angle with angle of attack. Flaps deflected 56.2°.

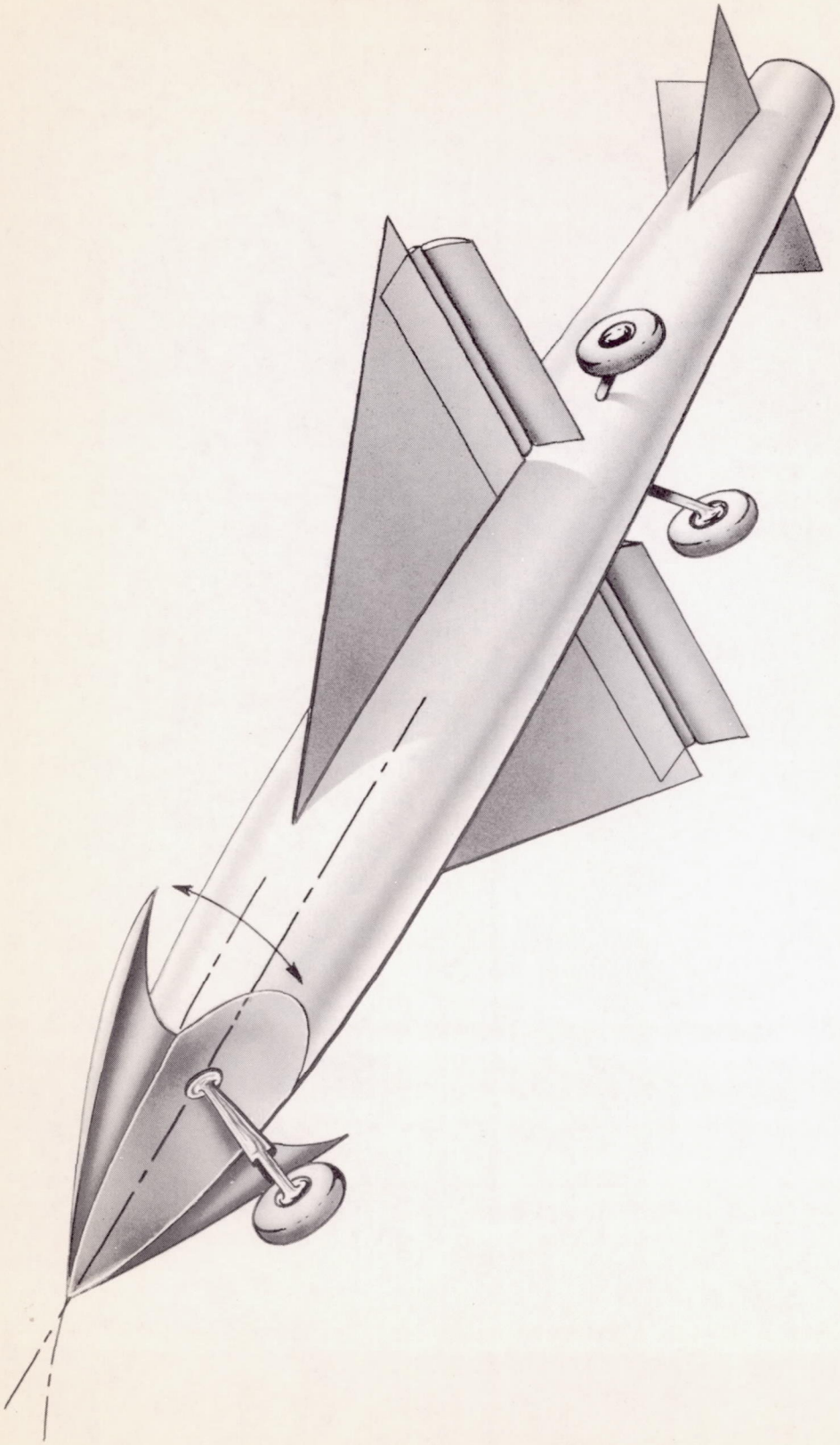

L-81276

Figure 16.- Retractable canard arrangement on a delta-wing airplane with extended double slotted flaps.

NACA-Langley - 1-5-54 - 325